

Triply heavy baryon spectroscopy revisited

Hao Zhou^{1,2,4}, Si-Qiang Luo^{1,2,4}^{*} and Xiang Liu^{1,2,3,4}[†]

¹School of Physical Science and Technology, Lanzhou University, Lanzhou 730000, China

²Lanzhou Center for Theoretical Physics, Key Laboratory of Theoretical Physics of Gansu Province,

Key Laboratory of Quantum Theory and Applications of MoE,

Gansu Provincial Research Center for Basic Disciplines of Quantum Physics, Lanzhou University, Lanzhou 730000, China

³MoE Frontiers Science Center for Rare Isotopes, Lanzhou University, Lanzhou 730000, China

⁴Research Center for Hadron and CSR Physics, Lanzhou University & Institute of Modern Physics of CAS, Lanzhou 730000, China

We present a comprehensive study of triply heavy baryons (Ω_{ccc} , Ω_{bbb} , Ω_{bcc} , and Ω_{bbc}) within the nonrelativistic quark model, employing the Gaussian expansion method to calculate mass spectra up to D -wave states. Our analysis represents the most complete treatment to date for this model, incorporating full angular momentum mixing effects. While our predictions for low-lying states agree well with lattice QCD results, we find systematically lower masses for excited states compared to lattice calculations. Using the obtained wave functions, we estimate radiative decay widths up to $1D$ states, revealing significant differences from previous theoretical work. Additionally, we identify and resolve several misconceptions in prior treatments of triply heavy baryon spectroscopy, particularly symmetry constraint and wave function construction in three-quark systems. These results provide crucial information for future experimental searches and theoretical investigations of triply heavy baryon systems.

I. INTRODUCTION

Hadron spectroscopy is an effective approach to deepen our understanding of the non-perturbative behavior of the strong interaction, a challenging task in contemporary particle physics. With the accumulation of experimental data over the past two decades, numerous new hadronic states have been observed [1–10]. The study of hadron spectroscopy is entering a new period, in which the characterization of conventional hadrons and the exploration of exotic hadronic states are becoming central research focuses.

Although the existence of triply heavy baryons is theoretically inevitable, the hunt for them is still underway, since they require the simultaneous production and binding of three heavy quarks, making their formation exceedingly rare. In 2017, the observation of the double-charm baryon $\Xi_{cc}^{++}(3621)$ by the LHCb Collaboration [11] raised expectations for new progress in the search for triply charmed baryons, especially with the upcoming high-luminosity upgrade of the LHC.

In fact, initial research on the spectroscopy of triply heavy baryons dates back to the bag model in 1980s [12, 13]. Later, the mass spectra of triply heavy baryons have been extensively studied using various theoretical frameworks, including relativistic or nonrelativistic quark model [14–29], lattice QCD [30–49], potential nonrelativistic QCD (pNRQCD) [50, 51], QCD sum rules [52–58], Regge phenomenology [59–61] and others [62–65]. These continued investigations also underscore the persistent attention given to triply heavy baryons in hadron physics.

Among these theoretical studies, Refs. [15–21, 23, 24, 28] focus exclusively on the low-lying states of triply heavy baryons, whereas Refs. [14, 22, 25–27, 29] provide systematic calculations of their mass spectra. Nevertheless, these

comprehensive investigations remain incomplete. For example, the interaction potentials used in Refs. [14, 25] include only central terms, making them unable to describe the fine structure of triply heavy baryons. Furthermore, the calculation in Ref. [26] neglected spin $S = 1/2$ and $S = 3/2$ state mixing—an omission that significantly impacts radiative decay computations—and was limited to the mass spectra of Ω_{ccc} and Ω_{bbb} baryons. Additionally, Ref. [27] employs a quark-diquark model, whereas Ref. [22] uses the hyperspherical approximation. Finally, Ref. [29] utilized only a single incomplete set of Jacobi coordinates and omitted decay studies. Given these limitations, a renewed investigation into the spectroscopy of triply heavy baryons—particularly higher-precision hadron spectroscopy—is warranted.

Over the past several years, we have successfully established theoretical descriptions of the mass spectra and decay properties of singly heavy baryons [66–68] and Ω hyperons [69] within the nonrelativistic quark model framework, additionally predicting new hadronic state [70]. These studies demonstrate that the effective potential employed in these works accurately reproduces hadronic spectroscopy. This validated formalism will now be extended to the present study of triply heavy baryons.

Triply heavy baryons constitute few-body systems. To address such systems with high precision, we employ the Gaussian Expansion Method (GEM) [71–73]. In this approach, the wave function of a few-body system is expanded into a set of Gaussian basis functions, transforming the solution of the stationary Schrödinger equation into a generalized eigenvalue problem. The Gaussian basis functions incorporate different angular momentum excitations, and the relative contributions of these excitations vary across different states and systems. Notably, a recent study [29] observed that the lowest state of the Ω_{bcc} baryon is dominated by the λ -mode, whereas the Ω_{bbc} baryon exhibits a dominant ρ -mode orbital excitation. In fact, this phenomenon was found and explained by Ref. [74] as early as 2015. We will investigate this phenomenon further from a symmetry perspective. Additionally, we will comprehen-

* luosq15@lzu.edu.cn

† xiangliu@lzu.edu.cn

sively account for angular momentum mixing effects—such as between total spin states ($S = 1/2$ and $S = 3/2$) and S - D mixing—to improve the description of the system's fine structure. Finally, we will address minor inaccuracies in earlier treatments of three-body systems composed of identical particles [25, 26, 29].

Owing to their high strong decay thresholds, triply heavy baryons are expected to decay predominantly via radiative transitions. However, only a limited number of studies [26, 28] have systematically calculated their radiative decay widths. Here, we present a systematic calculation of these decays. The nonrelativistic radiative decay framework, originally developed in Refs. [75–77], successfully described the radiative decays of charmonium and bottomonium by employing a multipole expansion of electromagnetic interactions (E_l and M_l transitions). In our work, we calculate the full transition amplitude directly, bypassing the multipole expansion, thereby achieving greater accuracy within the nonrelativistic approximation.

We note that Ref. [26] neglected the mixing between total spin states ($S = 1/2$ and $S = 3/2$) in its mass spectrum calculations. This omission is significant because the total spin S of the initial and final baryons determines whether an electric transition is allowed, directly influencing the radiative decay width. Furthermore, the wave function of a baryon composed of three identical quarks must adhere to fermionic symmetry, leading to distinct behavior compared to other baryon types. We will analyze how these effects shape the radiative decay properties of triply heavy baryons.

This paper is organized as follows. Following the introduction, we provide a brief review of the theoretical framework used in this work (Sec. II). In Sec. III, we present numerical results for the mass spectra and radiative decays of the studied triply heavy baryons. Finally, we conclude with a summary.

II. THEORETICAL FRAMEWORK

This section outlines the model and methodology employed in our study. First, we derive the Hamiltonian and determine the model parameters for triply heavy baryons within the non-relativistic quark model. Next, we construct the corresponding wave functions. We then numerically solve the stationary Schrödinger equation using the GEM. Finally, we utilize the obtained wave functions to calculate radiative decay widths of triply heavy baryons.

A. Effective Hamiltonian

In the conventional quark model framework, triply heavy baryons are composed of three heavy quarks. Following previous works [66–70], we adopt the same Hamiltonian, which is derived from the nonrelativistic limit of the formalism presented in Refs. [78, 79]. The Hamiltonian is taken as the

form:

$$H = \sum_i \left(m_i + \frac{p_i^2}{2m_i} \right) + \sum_{i < j} \left(V_{ij}^{\text{conf}} + V_{ij}^{\text{hyp}} + V_{ij}^{\text{so(cm)}} + V_{ij}^{\text{so(tp)}} \right). \quad (1)$$

Here, the potential energy component of the Hamiltonian comprises four distinct terms: (1) the confinement potential V_{ij}^{conf} , which governs quark confinement; (2) the hyperfine potential V_{ij}^{hyp} , responsible for inducing S - D wave mixing; (3) the color-magnetic potential $V_{ij}^{\text{so(cm)}}$, describing spin-orbit coupling effects; and (4) the Thomas precession potential $V_{ij}^{\text{so(tp)}}$, arising from relativistic dynamical corrections. These potentials take the following explicit forms:

$$V_{ij}^{\text{conf}} = -\frac{2}{3} \frac{\alpha_s}{r_{ij}} + \frac{b}{2} r_{ij} + \frac{1}{2} C, \quad (2)$$

$$V_{ij}^{\text{hyp}} = \frac{2\alpha_s}{3m_i m_j} \left[\frac{8\pi}{3} \tilde{\delta}(r_{ij}) \mathbf{S}_i \cdot \mathbf{S}_j + \frac{1}{r_{ij}^3} S(\mathbf{r}_{ij}, \mathbf{S}_i, \mathbf{S}_j) \right], \quad (3)$$

$$V_{ij}^{\text{so(cm)}} = \frac{2\alpha_s}{3r_{ij}^3} \left(\frac{\mathbf{r}_{ij} \times \mathbf{p}_i \cdot \mathbf{S}_i}{m_i^2} - \frac{\mathbf{r}_{ij} \times \mathbf{p}_j \cdot \mathbf{S}_j}{m_j^2} - \frac{\mathbf{r}_{ij} \times \mathbf{p}_j \cdot \mathbf{S}_i - \mathbf{r}_{ij} \times \mathbf{p}_i \cdot \mathbf{S}_j}{m_i m_j} \right), \quad (4)$$

$$V_{ij}^{\text{so(tp)}} = -\frac{1}{2r_{ij}} \frac{\partial V_{ij}^{\text{conf}}}{\partial r_{ij}} \left(\frac{\mathbf{r}_{ij} \times \mathbf{p}_i \cdot \mathbf{S}_i}{m_i^2} - \frac{\mathbf{r}_{ij} \times \mathbf{p}_j \cdot \mathbf{S}_j}{m_j^2} \right), \quad (5)$$

$$\tilde{\delta}(r_{ij}) = \frac{\sigma^3}{\pi^{3/2}} e^{-\sigma^2 r_{ij}^2}, \quad S(\mathbf{r}_{ij}, \mathbf{S}_i, \mathbf{S}_j) = \frac{3\mathbf{S}_i \cdot \mathbf{r}_{ij} \mathbf{S}_j \cdot \mathbf{r}_{ij}}{r_{ij}^2} - \mathbf{S}_i \cdot \mathbf{S}_j, \quad (6)$$

where m_i , \mathbf{p}_i , and \mathbf{S}_i represent the mass, center-of-mass momentum, and spin of the i -th quark respectively, while $\mathbf{r}_{ij} = \mathbf{r}_i - \mathbf{r}_j$ denotes the relative position vector between the i -th and j -th quarks.

The parameters of the model include: α_s (one-gluon-exchange coupling constant), b (linear confinement strength), C (renormalized mass constant), and σ (smearing parameter). All parameters are listed in Table I, with separate parameter sets used for cc , cb , and bb interactions.

The parameter determination was performed as follows: the charm quark mass m_c and first row parameters are obtained by fitting the charmonium spectrum; the bottom quark mass m_b and last row parameters are determined from bottomonium spectrum fits; while the middle row parameters are derived through B_c meson mass spectrum fitting.

B. Wave function

To determine the mass spectra of triply heavy baryons, we should solve the stationary Schrödinger equation corresponding to the Hamiltonian in Eq. (1). Prior to numerical solution,

TABLE I. The parameters involved in the adopted potential model.

	α_s	$b(\text{GeV}^2)$	$C(\text{GeV})$	$\sigma(\text{GeV})$
cc	0.470	0.165	-0.409	1.220
cb	0.362	0.189	-0.555	1.586
bb	0.333	0.203	-0.603	1.908
$m_c = 1.649 \text{ GeV}$				$m_b = 5.036 \text{ GeV}$

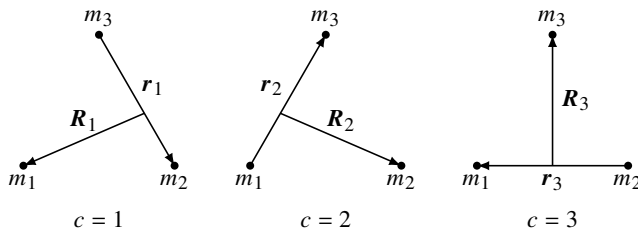


FIG. 1. Three Jacobian coordinates of three-body system.

we can identify operators that commute with the Hamiltonian to construct a complete set of commuting observables. This approach provides preliminary insights into the wave function's structure.

For the angular momentum components, we naturally select operators corresponding to L - S coupling. The final results are, in principle, independent of the chosen coupling representation. The operator set is

$$\{l_c^2, L_c^2, L^2, S_1^2, S_2^2, S_3^2, S_{ij}^2, S^2, J^2, J_z\}, \quad (7)$$

where \mathbf{l}_c and \mathbf{L}_c represent the orbital angular momenta associated with the c -th Jacobi coordinates \mathbf{r}_c and \mathbf{R}_c , respectively, while \mathbf{S}_1 , \mathbf{S}_2 , and \mathbf{S}_3 denote the spins of the constituent quarks m_1 , m_2 , and m_3 , as illustrated in Fig. 1. The composite angular momenta are defined as:

- $\mathbf{L} = \mathbf{l}_c + \mathbf{L}_c$ (total orbital angular momentum),
- $\mathbf{S}_{ij} = \mathbf{S}_i + \mathbf{S}_j$ (pair spin in \mathbf{r}_c -degree-of-freedom),
- $\mathbf{S} = \mathbf{S}_1 + \mathbf{S}_2 + \mathbf{S}_3$ (total spin),
- $\mathbf{J} = \mathbf{L} + \mathbf{S}$ (total angular momentum).

We first examine the commutation relations between these operators (Eq. (7)) and the Hamiltonian. Notably, l_c^2 and L_c^2 fail to commute with the central potential $V_{ij}(r_{ij})$, requiring the system's wave function to be expressed as a superposition of states with different l_c and L_c quantum numbers. However, \mathbf{L} does commute with both $V_{ij}(r_{ij})$ and the dominant spin-spin interaction terms $\mathbf{S}_i \cdot \mathbf{S}_j$, making L a reasonably good quantum number. Our subsequent calculations will demonstrate that the S - D mixing effect is indeed negligible.

For any given L , there exist infinitely many possible couplings between l_c and L_c . Following established approaches [71], we employ an expansion using Jacobian coordinates of three rearrangement channels ($c = 1 \sim 3$) while restricting l_c and L_c to relatively small values. As demonstrated in previous studies [72, 73], this treatment ensures rapid convergence

of mass and binding energy calculations due to the inherent advantages of three-channel Jacobi coordinates.

The operator S_{ij}^2 commutes exclusively with the contact term $\mathbf{S}_i \cdot \mathbf{S}_j$ and the tensor term $S(\mathbf{r}_{ij}, \mathbf{S}_i, \mathbf{S}_j)$, whereas S^2 only commutes with $\mathbf{S}_i \cdot \mathbf{S}_j$ —a notable departure from two-body systems. Consequently, the non-commuting terms with S_{ij}^2 and S^2 necessitate the wave function to be a superposition of states with different s_{ij} and S quantum numbers. The total angular momentum \mathbf{J} , being fully conserved (i.e., commuting with the Hamiltonian), serves as the primary quantum number for state classification.

Finally, we discuss a special case where a matrix element vanishes due to symmetry considerations. This case is helpful for understanding the mixing of different modes. If V remains unchanged under the transformation $\mathbf{r}_c \rightarrow -\mathbf{r}_c$ or $\mathbf{R}_c \rightarrow -\mathbf{R}_c$, then the matrix element

$$\langle l'_c L'_c L' M' | V | l_c L_c LM \rangle = (-1)^{l'_c + l_c} \langle l'_c L'_c L' M' | V | l_c L_c LM \rangle \quad (8)$$

or

$$\langle l'_c L'_c L' M' | V | l_c L_c LM \rangle = (-1)^{L'_c + L_c} \langle l'_c L'_c L' M' | V | l_c L_c LM \rangle. \quad (9)$$

This shows that the matrix element of V is not zero only when $l'_c + l_c = \text{even}$ or $L'_c + L_c = \text{even}$, so V can only lead to the mixing of bases of $l'_c + l_c = \text{even}$ or $L'_c + L_c = \text{even}$. The confinement and hyperfine potential of the Ω_{bcc} and Ω_{bbc} baryons precisely satisfy transformation invariance, so the mixing of different modes of most of their states is relatively small. But the (0,2,2)-mode and (2,0,2)-mode may form a large mixing.

C. Gaussian expansion method

The system described by Hamiltonian H satisfies the stationary Schrödinger equation

$$H\Psi = E\Psi. \quad (10)$$

We expand the total wave function in terms of a complete set of L^2 -integrable basis functions Φ_α , where α denotes the set of quantum numbers labeling each basis state:

$$\Psi = \sum_{\alpha} C_{\alpha} \Phi_{\alpha}. \quad (11)$$

Applying the Rayleigh-Ritz variational principle yields a generalized matrix eigenvalue problem:

$$HC = NCE, \quad (12)$$

where the Hamiltonian and overlap matrix elements are respectively given by

$$H_{\alpha'\alpha} = \langle \Phi_{\alpha'} | H | \Phi_{\alpha} \rangle, \quad (13)$$

$$N_{\alpha'\alpha} = \langle \Phi_{\alpha'} | \Phi_{\alpha} \rangle. \quad (14)$$

The GEM employs carefully selected Gaussian basis functions that form an approximately complete set in finite coordinate space. This choice enables accurate description of both

TABLE II. LS -coupling scheme in the three-body angular-momentum space for triply heavy baryons. Parameters r_{\min} , r_{\max} , R_{\min} , and R_{\max} are in fm.

J^P	l	L	L_t	s_{ij}	S	n_{\max}	r_{\min}	r_{\max}	N_{\max}	R_{\min}	R_{\max}
$\frac{1}{2}^+$	0	0	0	1	$\frac{1}{2}$	10	0.1	5.0	10	0.1	5.0
	1	1	0	0	$\frac{1}{2}$	10	0.1	5.0	10	0.1	5.0
$\frac{3}{2}^+$	0	2	2	1	$\frac{3}{2}$	10	0.1	5.0	10	0.1	5.0
	2	0	2	1	$\frac{3}{2}$	10	0.1	5.0	10	0.1	5.0
	1	1	1	0	$\frac{1}{2}$	10	0.1	5.0	10	0.1	5.0
	2	2	1	1	$\frac{1}{2}$	10	0.1	5.0	10	0.1	5.0
$\frac{5}{2}^+$	0	0	0	1	$\frac{3}{2}$	10	0.1	5.0	10	0.1	5.0
	2	2	0	1	$\frac{3}{2}$	10	0.1	5.0	10	0.1	5.0
	0	2	2	1	$\frac{3}{2}$	10	0.1	5.0	10	0.1	5.0
	2	0	2	1	$\frac{3}{2}$	10	0.1	5.0	10	0.1	5.0
	2	0	2	1	$\frac{1}{2}$	10	0.1	5.0	10	0.1	5.0
	1	1	2	0	$\frac{1}{2}$	10	0.1	5.0	10	0.1	5.0
	0	2	2	1	$\frac{1}{2}$	10	0.1	5.0	10	0.1	5.0
	1	1	1	0	$\frac{1}{2}$	10	0.1	5.0	10	0.1	5.0
	2	2	1	1	$\frac{1}{2}$	10	0.1	5.0	10	0.1	5.0
	2	2	1	1	$\frac{3}{2}$	10	0.1	5.0	10	0.1	5.0
$\frac{7}{2}^+$	0	2	2	1	$\frac{3}{2}$	10	0.1	5.0	10	0.1	5.0
	2	0	2	1	$\frac{3}{2}$	10	0.1	5.0	10	0.1	5.0
	2	0	2	1	$\frac{1}{2}$	10	0.1	5.0	10	0.1	5.0
	1	1	2	0	$\frac{1}{2}$	10	0.1	5.0	10	0.1	5.0
	0	2	2	1	$\frac{1}{2}$	10	0.1	5.0	10	0.1	5.0
	2	2	1	1	$\frac{3}{2}$	10	0.1	5.0	10	0.1	5.0
	2	2	3	1	$\frac{3}{2}$	10	0.1	5.0	10	0.1	5.0
	1	3	3	0	$\frac{1}{2}$	10	0.1	5.0	10	0.1	5.0
	2	2	3	1	$\frac{1}{2}$	10	0.1	5.0	10	0.1	5.0
	3	1	3	0	$\frac{1}{2}$	10	0.1	5.0	10	0.1	5.0
$\frac{1}{2}^-$	0	1	1	1	$\frac{1}{2}$	10	0.1	5.0	10	0.1	5.0
	1	0	1	0	$\frac{1}{2}$	10	0.1	5.0	10	0.1	5.0
	0	1	1	1	$\frac{3}{2}$	10	0.1	5.0	10	0.1	5.0
	2	1	2	1	$\frac{3}{2}$	10	0.1	5.0	10	0.1	5.0
	0	1	1	1	$\frac{1}{2}$	10	0.1	5.0	10	0.1	5.0
	1	0	1	0	$\frac{1}{2}$	10	0.1	5.0	10	0.1	5.0
	0	1	1	1	$\frac{3}{2}$	10	0.1	5.0	10	0.1	5.0
	2	1	3	1	$\frac{3}{2}$	10	0.1	5.0	10	0.1	5.0
	1	2	2	0	$\frac{1}{2}$	10	0.1	5.0	10	0.1	5.0
	2	1	2	1	$\frac{1}{2}$	10	0.1	5.0	10	0.1	5.0
$\frac{3}{2}^-$	0	1	1	1	$\frac{3}{2}$	10	0.1	5.0	10	0.1	5.0
	0	3	3	1	$\frac{3}{2}$	10	0.1	5.0	10	0.1	5.0
	1	2	3	0	$\frac{1}{2}$	10	0.1	5.0	10	0.1	5.0
	2	1	3	1	$\frac{1}{2}$	10	0.1	5.0	10	0.1	5.0
	3	0	3	0	$\frac{1}{2}$	10	0.1	5.0	10	0.1	5.0
	0	3	3	1	$\frac{1}{2}$	10	0.1	5.0	10	0.1	5.0
	2	1	3	1	$\frac{3}{2}$	10	0.1	5.0	10	0.1	5.0
	1	2	2	0	$\frac{1}{2}$	10	0.1	5.0	10	0.1	5.0
	2	1	2	1	$\frac{1}{2}$	10	0.1	5.0	10	0.1	5.0
	2	1	2	1	$\frac{3}{2}$	10	0.1	5.0	10	0.1	5.0
$\frac{5}{2}^-$	0	1	1	1	$\frac{3}{2}$	10	0.1	5.0	10	0.1	5.0
	0	3	3	1	$\frac{3}{2}$	10	0.1	5.0	10	0.1	5.0
	1	2	3	0	$\frac{1}{2}$	10	0.1	5.0	10	0.1	5.0
	2	1	3	1	$\frac{1}{2}$	10	0.1	5.0	10	0.1	5.0
	3	0	3	0	$\frac{1}{2}$	10	0.1	5.0	10	0.1	5.0
	0	3	3	1	$\frac{1}{2}$	10	0.1	5.0	10	0.1	5.0
	2	1	3	1	$\frac{3}{2}$	10	0.1	5.0	10	0.1	5.0
	1	2	2	0	$\frac{1}{2}$	10	0.1	5.0	10	0.1	5.0
	2	1	2	1	$\frac{1}{2}$	10	0.1	5.0	10	0.1	5.0
	2	1	2	1	$\frac{3}{2}$	10	0.1	5.0	10	0.1	5.0

short-range correlations and long-range asymptotic behavior, as well as the highly oscillatory nature of wave functions in bound and scattering states [72].

For Ω_{ccc} and Ω_{bbb} systems, accounting for the symmetry

of three identical quarks, we construct the basis functions as:

$$\Phi_\alpha = [[\phi_{nl}^G(\mathbf{r}_1)\phi_{NL}^G(\mathbf{R}_1)]_{L_t}[s_1[s_2s_3]_{S_{23}}]_S]_{JM} + [[\phi_{nl}^G(\mathbf{r}_2)\phi_{NL}^G(\mathbf{R}_2)]_{L_t}[s_2[s_3s_1]_{S_{31}}]_S]_{JM} + [[\phi_{nl}^G(\mathbf{r}_3)\phi_{NL}^G(\mathbf{R}_3)]_{L_t}[s_3[s_1s_2]_{S_{12}}]_S]_{JM}. \quad (15)$$

For Ω_{bcc} and Ω_{bbc} systems, with two identical quarks positioned at m_2 and m_3 in Fig. 1, we use the symmetric basis:

$$\Phi_\alpha = [[\phi_{nl}^G(\mathbf{r}_1)\phi_{NL}^G(\mathbf{R}_1)]_{L_t}[s_1[s_2s_3]_{S_{23}}]_S]_{JM}, \quad (16)$$

where $\alpha = \{l, L, L_t, s_{ij}, S, n, N\}$. The quantum numbers used for each J^P state are listed in Table II. Here we simplify notation by abbreviating l_c and L_c to l and L (due to identical particle symmetry) and denote the total orbital angular momentum as L_t to avoid confusion.

The spatial components of Eqs. (15) and (16) employ Gaussian basis functions of the form:

$$\phi_{nlm}^G(\mathbf{r}) = \tilde{\phi}_{nl}^G(r)Y_{lm}(\hat{\mathbf{r}}), \quad \tilde{\phi}_{nl}^G(r) = N_{nl}r^l e^{-\nu_n r^2}, \\ \phi_{NLM}^G(\mathbf{R}) = \tilde{\phi}_{NL}^G(R)Y_{LM}(\hat{\mathbf{R}}), \quad \tilde{\phi}_{NL}^G(R) = N_{NL}R^L e^{-\lambda_N R^2}, \quad (17)$$

with normalization constants:

$$N_{nl} = \left(\frac{2^{l+2}(2\nu_n)^{l+\frac{3}{2}}}{\sqrt{\pi}(2l+1)!!} \right)^{\frac{1}{2}}, \quad N_{NL} = \left(\frac{2^{L+2}(2\lambda_N)^{L+\frac{3}{2}}}{\sqrt{\pi}(2L+1)!!} \right)^{\frac{1}{2}}, \quad (18)$$

and Gaussian range parameters:

$$\nu_n = 1/r_n^2, \quad r_n = r_1 a^{n-1} \quad (n = 1 \sim n_{\max}), \\ \lambda_N = 1/R_N^2, \quad R_N = R_1 A^{N-1} \quad (N = 1 \sim N_{\max}). \quad (19)$$

Empirical evidence suggests that geometric progression provides optimal Gaussian size parameters.

The basis functions Φ_α are constrained by:

- Total angular momentum and parity conservation (J^P),
 - Symmetrization requirements for identical particles,
 - Hamiltonian commutation relations.
- For given J^P , Φ_α must satisfy:
- Angular momentum coupling: $|L_t - S| \leq J \leq L_t + S$,
 - Parity: $P = (-1)^{l+L}$,
 - Symmetry condition: $l + s_{ij} = \text{odd}$ (from symmetrization requirements).

The tensor and spin-orbit terms leading to the mixing of different L_t and S can be expressed as irreducible tensors:

$$S(\mathbf{r}_{ij}, \mathbf{S}_i, \mathbf{S}_j) = \sqrt{24\pi} \left(Y_2(\hat{\mathbf{r}}_{ij}) \otimes (S_i^{(1)} \otimes S_j^{(1)})^{(2)} \right)_0^{(0)}, \quad (20)$$

$$\mathbf{L} \cdot \mathbf{S} = -\sqrt{3} (L^{(1)} \otimes S^{(1)})_0^{(0)}, \quad (21)$$

where \mathbf{L} and \mathbf{S} correspond to any $\mathbf{r} \times \mathbf{p}$ and \mathbf{S}_k in $V_{ij}^{\text{so(cm)}}$ and $V_{ij}^{\text{so(tp)}}$.

The energy matrix elements (Eq. (13)) decompose into spatial and spin components via:

$$\begin{aligned} & \langle j'_1 j'_2 j' m' | (T_1^{(k_1)} \otimes T_2^{(k_2)})_q^{(k)} | j_1 j_2 j m \rangle = \\ & (-1)^{j'-m'} \begin{pmatrix} j' & k & j \\ -m' & q & m \end{pmatrix} \sqrt{(2j'+1)(2k+1)(2j+1)} \\ & \left\{ \begin{matrix} j'_1 & j_1 & k_1 \\ j'_2 & j_2 & k_2 \\ j' & j & k \end{matrix} \right\} \langle j'_1 \| T_1^{(k_1)} \| j_1 \rangle \langle j'_2 \| T_2^{(k_2)} \| j_2 \rangle, \end{aligned} \quad (22)$$

where $(j'_1 k_1 j_1)$ and $(j'_2 k_2 j_2)$ must satisfy triangular conditions.

For different terms, non-vanishing matrix elements require:

- Tensor/spin-orbit terms: $|L'_t - L_t| \leq 2/1 \leq L'_t + L_t$ and $|S' - S| \leq 2/1 \leq S' + S$,
- Commuting terms with L^2 and S^2 : $L'_t = L_t$ and $S' = S$.

In practice, we consider only $L_t \leq 3$ for $J^P = \frac{1}{2}^\pm, \frac{3}{2}^\pm, \frac{5}{2}^\pm, \frac{7}{2}^+$, neglecting higher orbital excitations. Table II summarizes the allowed quantum numbers and Gaussian ranges for each J^P state of triply heavy baryons.

D. Radiative decay formalism

Using the obtained wave functions of triply heavy baryons, we can calculate their radiative decay properties. The theoretical framework for calculating radiative decays within the non-relativistic constituent quark model has been well established in Refs. [75–77], and this formalism has been successfully applied to various systems [68]. Below we briefly summarize the key steps of the calculation.

The quark-photon electromagnetic interaction at tree level is described by

$$H_e = - \sum_j e_j \bar{\psi}_j \gamma_\mu^j A^\mu(\mathbf{k}, \mathbf{r}) \psi_j, \quad (23)$$

where ψ_j represents the field of the j -th quark in the hadron, e_j and γ_μ^j denote the electric charge and Dirac matrices of the constituent quark ψ_j , and $A^\mu(\mathbf{k}, \mathbf{r})$ is the photon field.

In the nonrelativistic limit, this interaction simplifies to

$$h_e \approx \sum_j \left[e_j \mathbf{r}_j \cdot \boldsymbol{\epsilon} - \frac{e_j}{2m_j} \boldsymbol{\sigma}_j \cdot (\boldsymbol{\epsilon} \times \hat{\mathbf{k}}) \right] e^{-i\mathbf{k} \cdot \mathbf{r}_j}, \quad (24)$$

where m_j , e_j , $\boldsymbol{\sigma}_j$, and \mathbf{r}_j are the mass, charge, Pauli matrices, and position of the j -th quark, respectively. The \mathbf{k} and $\boldsymbol{\epsilon}$ in Eq. (24) represent the momentum and polarization vector of the photon, respectively.

The corresponding helicity amplitude for the electromagnetic transition is given by

$$\mathcal{A} = -i \sqrt{\frac{\omega_\gamma}{2}} \langle f | h_e | i \rangle, \quad (25)$$

where $\langle f |$ and $| i \rangle$ denote the wave functions of the final and initial baryon states, respectively. The $\omega_\gamma = (M_i^2 - M_f^2)/(2M_i)$

in Eq. (25) is the photon energy, where M_i and M_f are the masses of the initial and final baryons, respectively. We choose the coordinate system such that the photon momentum aligns with the z -axis ($\mathbf{k} = (0, 0, \omega_\gamma)$) and take the polarization vector as $\boldsymbol{\epsilon} = (1, i, 0)/\sqrt{2}$.

The radiative decay width is then obtained from the helicity amplitude through

$$\Gamma = \frac{|\mathbf{k}|^2}{\pi} \frac{2}{2J_i + 1} \frac{M_f}{M_i} \sum_{J_{fz}, J_{iz}} |\mathcal{A}_{J_{fz}, J_{iz}}|^2, \quad (26)$$

where J_i is the total angular momentum of the initial baryon, and J_{iz} and J_{fz} are the z -components of the angular momenta for the initial and final states, respectively.

III. NUMERICAL RESULTS

A. Mass spectra

Using the GEM to numerically solve the stationary Schrödinger equation for triply heavy baryons, we obtain the mass spectra shown in Fig. 2, where we compare our results with lattice QCD calculations. The numerical values of the masses and angular momentum excitation proportions are presented in Tables III and IV, with lattice results provided in Table V for reference.

In the absence of experimental data, we compare our results with lattice QCD calculations. For Ω_{ccc} baryons, most lattice studies have focused on the low-lying states with $J^P = \frac{3}{2}^+$ and $\frac{3}{2}^-$, with only Ref. [31] providing spectra up to $J^P = \frac{7}{2}^+$. For the $\frac{3}{2}^\pm$ states, we use the most recent lattice results from Ref. [30], which claims to fully account for systematic uncertainties, while other J^P states are compared with Ref. [31].

For Ω_{bcc} and Ω_{bbc} baryons, only three lattice studies [32–34] have calculated masses for the low-lying $J^P = \frac{1}{2}^\pm$ and $\frac{3}{2}^\pm$ states (Table V). In Fig. 2, we plot only the results from Ref. [32] due to their consistency with other calculations. For Ω_{bbb} baryons, the most recent published results [33] are a decade old, with highly excited states reported only in Refs. [35, 36]. We omit the results from Ref. [34] from the figure due to their larger uncertainties, though they are included in Table V for completeness.

1. Ω_{ccc} and Ω_{bbb} baryons

The upper panel of Fig. 2 displays our predicted mass spectra for Ω_{ccc} and Ω_{bbb} baryons with quantum numbers $J^P = \frac{1}{2}^\pm, \frac{3}{2}^\pm, \frac{5}{2}^\pm$, and $\frac{7}{2}^+$. For these two kinds of baryons, our predictions for the lowest $\frac{3}{2}^+, \frac{1}{2}^-$ and $\frac{3}{2}^-$ states agree well with the latest lattice results [30, 33], though other states show significant deviations from the only available lattice data [31, 36]. We note that the highly excited states in Ref. [31] carry substantial uncertainties, limiting their reliability as benchmarks.

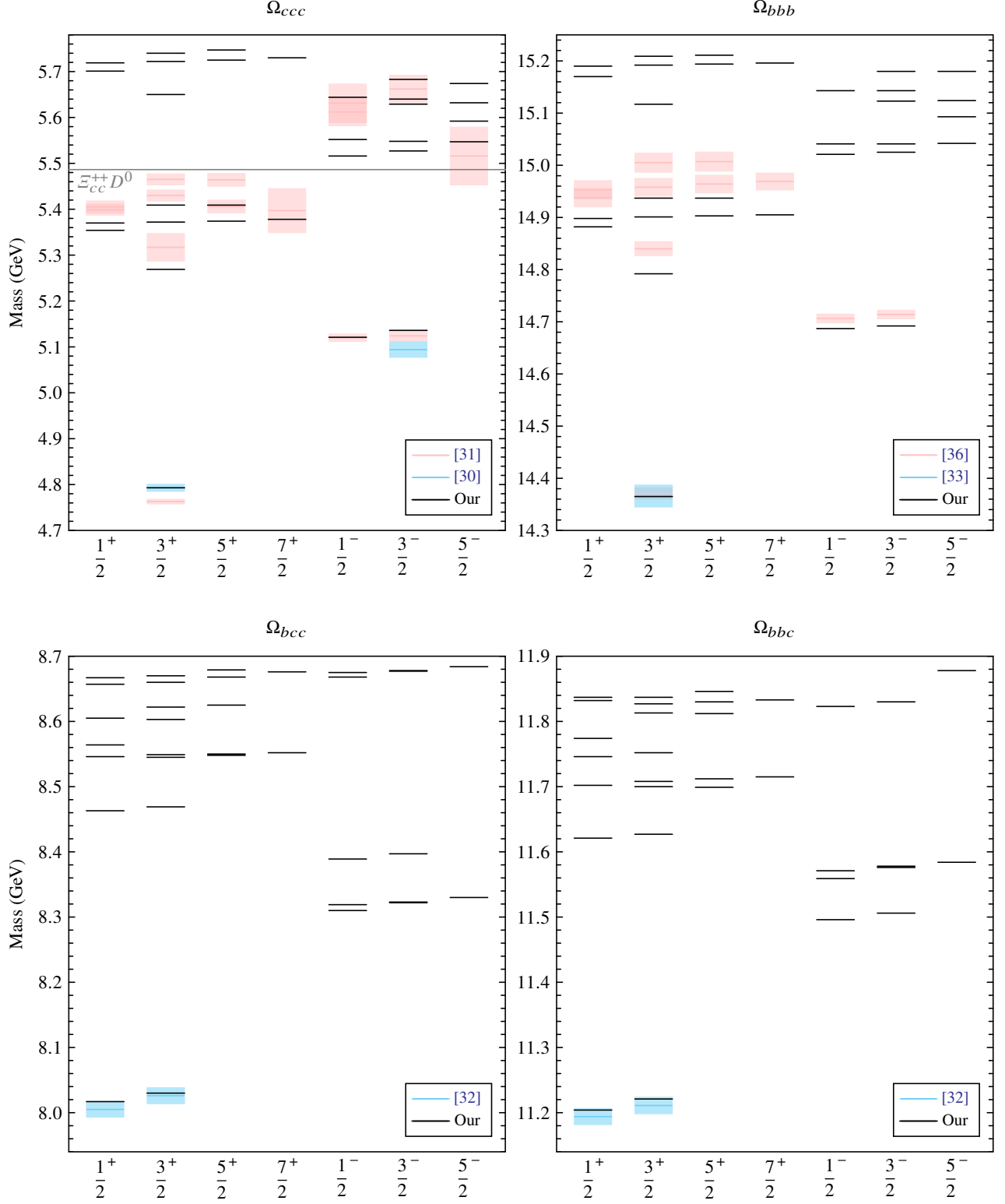


FIG. 2. The mass spectrum of triply heavy baryons. Here, blue and pink are the lattice results.

TABLE III. The mass spectra of the Ω_{ccc} and Ω_{bbb} baryons and the proportion of (L_t, S) in each state. The first two columns of the table correspond one-to-one with Table II. The first eight radial excitations of triply heavy baryons with a given J^P are listed in the row where the symbol (L_t, S) is located in MeV. The numbers under each radial excitation represent the proportion of (L_t, S) corresponding to the row where the number is located. The maximum number in each column has been bolded.

J^P	(L_t, S)	Ω_{ccc}								Ω_{bbb}							
		5354	5370	5701	5719	5784	5851	5885	6011	14882	14898	15170	15190	15257	15324	15349	15424
	$(0, \frac{1}{2})$	97.34	2.59	98.11	1.80	99.43	0.55	0.03	98.55	99.83	0.17	99.90	0.09	99.99	0.01	0.01	99.92
1^+	$(2, \frac{3}{2})$	2.66	97.38	1.86	98.09	0.14	3.58	96.35	1.38	0.17	99.83	0.10	99.90	0.01	0.08	99.91	0.07
$\frac{1}{2}$	$(1, \frac{1}{2})$	0.00	0.02	0.04	0.10	0.43	95.87	3.61	0.06	0.00	0.00	0.00	0.01	99.91	0.08	0.00	
	$(1, \frac{3}{2})$	0.00	0.01	0.00	0.00	0.00	0.00	0.01	0.01	0.00	0.00	0.00	0.00	0.00	0.00	0.00	
J^P	(L_t, S)	4793	5269	5372	5409	5650	5722	5740	5796	14365	14792	14901	14937	15117	15192	15209	15266
	$(0, \frac{3}{2})$	99.78	99.79	0.06	0.03	99.71	0.11	0.05	0.02	99.98	99.98	0.00	0.00	99.98	0.01	0.00	0.00
	$(2, \frac{3}{2})$	0.12	0.13	97.41	2.48	0.19	96.44	3.17	0.31	0.01	0.01	99.93	0.06	0.01	99.94	0.04	0.01
3^+	$(2, \frac{1}{2})$	0.09	0.08	2.51	97.47	0.08	3.39	96.71	99.31	0.01	0.01	0.06	99.94	0.01	0.04	99.96	99.98
$\frac{1}{2}$	$(1, \frac{1}{2})$	0.00	0.00	0.01	0.00	0.02	0.04	0.05	0.35	0.00	0.00	0.00	0.00	0.00	0.00	0.01	
	$(1, \frac{3}{2})$	0.00	0.00	0.01	0.00	0.00	0.01	0.01	0.01	0.00	0.00	0.00	0.00	0.00	0.00	0.00	
	$(3, \frac{3}{2})$	0.00	0.00	0.01	0.01	0.00	0.01	0.01	0.01	0.00	0.00	0.00	0.00	0.00	0.00	0.00	
J^P	(L_t, S)	5374	5409	5725	5747	5801	5852	5883	5887	14903	14937	15194	15211	15267	15327	15351	15354
	$(2, \frac{3}{2})$	90.14	9.82	87.88	11.53	0.54	0.90	48.87	50.24	99.66	0.33	99.53	0.43	0.03	0.05	99.87	0.08
	$(2, \frac{1}{2})$	9.83	90.17	12.09	88.45	99.42	98.99	0.78	0.25	0.34	99.67	0.46	99.56	99.97	99.95	0.05	0.00
5^+	$(1, \frac{3}{2})$	0.00	0.00	0.00	0.00	0.00	0.00	0.00	0.00	0.00	0.00	0.00	0.00	0.00	0.00	0.00	
$\frac{1}{2}$	$(3, \frac{3}{2})$	0.01	0.00	0.01	0.01	0.00	0.00	0.00	0.01	0.00	0.00	0.00	0.00	0.00	0.00	0.00	
	$(3, \frac{1}{2})$	0.02	0.00	0.02	0.01	0.02	0.10	50.35	49.50	0.00	0.00	0.00	0.00	0.00	0.08	99.91	
J^P	(L_t, S)	5378	5730	5879	5891	6041	6131	6186	6200	14905	15196	15352	15356	15448	15538	15600	15608
	$(2, \frac{3}{2})$	99.99	99.96	59.87	40.14	99.93	99.83	9.28	85.18	100.0	100.0	95.09	4.91	100.0	100.0	0.67	99.28
7^+	$(3, \frac{3}{2})$	0.01	0.00	0.00	0.01	0.00	0.01	0.47	0.50	0.00	0.00	0.00	0.00	0.00	0.03	0.01	
$\frac{1}{2}$	$(3, \frac{1}{2})$	0.01	0.03	40.13	59.85	0.06	0.16	90.25	14.32	0.00	0.00	4.91	95.09	0.00	0.00	99.29	0.71
J^P	(L_t, S)	5121	5516	5552	5644	5854	5872	5958	5983	14687	15021	15041	15143	15299	15304	15398	15422
	$(1, \frac{1}{2})$	99.93	99.76	0.30	99.87	98.93	1.10	99.93	99.78	99.99	99.94	0.06	99.99	99.03	0.97	99.99	99.99
1^-	$(1, \frac{3}{2})$	0.04	0.22	99.67	0.12	1.05	98.86	0.05	0.16	0.00	0.06	99.93	0.01	0.97	99.02	0.00	0.01
$\frac{1}{2}$	$(2, \frac{3}{2})$	0.02	0.02	0.03	0.01	0.02	0.03	0.02	0.06	0.00	0.00	0.00	0.00	0.00	0.00	0.01	
J^P	(L_t, S)	5136	5527	5548	5629	5640	5683	5862	5868	14692	15025	15041	15123	15143	15180	15302	15304
	$(1, \frac{1}{2})$	99.90	99.00	1.21	5.11	93.61	0.98	87.24	12.79	99.99	99.92	0.08	0.05	99.92	0.02	96.91	3.09
	$(1, \frac{3}{2})$	0.00	0.87	98.67	0.01	0.34	0.05	12.58	87.09	0.00	0.07	99.90	0.00	0.01	0.01	3.08	96.90
3^-	$(3, \frac{3}{2})$	0.08	0.08	0.02	93.12	5.58	1.27	0.09	0.02	0.01	0.01	0.00	99.90	0.05	0.04	0.01	0.00
$\frac{1}{2}$	$(2, \frac{1}{2})$	0.00	0.03	0.07	1.76	0.46	97.69	0.07	0.07	0.00	0.00	0.01	0.04	0.02	99.92	0.00	0.01
	$(2, \frac{3}{2})$	0.02	0.01	0.03	0.00	0.01	0.01	0.02	0.03	0.00	0.00	0.00	0.00	0.00	0.00	0.00	
J^P	(L_t, S)	5547	5592	5632	5674	5868	5910	5930	5997	15042	15093	15124	15180	15305	15352	15364	15436
	$(1, \frac{3}{2})$	99.80	0.01	0.05	0.05	99.77	0.01	0.09	0.04	99.99	0.00	0.00	0.00	99.98	0.00	0.00	0.00
5^-	$(3, \frac{1}{2})$	0.06	99.27	0.51	0.23	0.06	98.09	2.32	49.69	0.01	99.99	0.00	0.01	99.96	0.07	95.30	
$\frac{1}{2}$	$(3, \frac{3}{2})$	0.07	0.40	97.69	1.84	0.10	1.67	97.34	20.95	0.01	0.00	99.94	0.05	0.01	0.03	99.92	4.50
	$(2, \frac{1}{2})$	0.06	0.32	1.74	97.87	0.06	0.22	0.24	29.29	0.00	0.01	0.05	99.93	0.00	0.01	0.01	0.20
	$(2, \frac{3}{2})$	0.01	0.01	0.00	0.01	0.01	0.02	0.04	0.00	0.00	0.00	0.00	0.00	0.00	0.00	0.00	

Despite these quantitative differences, both approaches predict qualitatively similar energy level structures.

In our model, Ω_{ccc} and Ω_{bbb} differ only in quark mass, resulting in nearly identical energy level structures (upper panel of Fig. 2). Table III reveals that most states are dominated by single total orbital angular momentum excitations (L_t), with minimal mixing between different L_t values. We therefore characterize states by their dominant orbital component (S, P, D):

- $\frac{1}{2}^+$ system: Contains two nearly degenerate S - D wave pairs, distinct from simple spin excitation pairs
- $\frac{3}{2}^+$ system: Features the ground states ($1S$), followed by $2S$ - $3S$ states and two $1D$ - $2D$ spin excitation pairs
- $\frac{5}{2}^+$ system: Shows two $1D$ - $2D$ pairs with moderate spin $S = 1/2$ and $S = 3/2$ state mixing

- $\frac{7}{2}^+$ system: Contains only D -wave states ($S = 3/2$ required for $J = 7/2$ coupling)
- Negative parity systems: Exhibit clean P -wave ($1P, 2P, 3P$) and F -wave patterns. A particularly interesting state appears in the $\frac{5}{2}^-$ system, where $L_t = 2$ emerges from coupled orbital angular momenta (1 and 2) as detailed in Table II.

We clarify a common misconception regarding $J^P = \frac{1}{2}^+$ states in three-identical-particle systems. Contrary to claims in Refs. [25, 29], S -wave bound states are indeed possible despite the Pauli principle. While no symmetric $S = 1/2$ spin state exists for three identical fermions, Eq. (15) demonstrates how symmetric spatial states can be constructed through appropriate combinations of two-particle symmetric states. This explains the presence of closely spaced S -wave and D -wave states in the $\frac{1}{2}^+$ channel of Ω_{ccc} and Ω_{bbb} mass spectra.

It is true that the $J^P = \frac{1}{2}^+$ S -wave states are also calculated

TABLE IV. The mass spectra of the Ω_{bcc} and Ω_{bbc} baryons and the proportion of (l, L, L_t, S) in each state.

J^P	(l, L, L_t, S)	Ω_{bcc}								Ω_{bbc}							
		8017	8463	8546	8564	8605	8657	8667	8825	11204	11621	11702	11746	11774	11832	11837	11948
$\frac{1}{2}^+$	$(0, 0, 0, \frac{1}{2})$	99.91	99.91	0.01	0.20	99.32	0.18	0.29	99.88	99.98	99.95	0.07	99.16	0.78	0.04	0.01	99.83
	$(1, 1, 0, \frac{1}{2})$	0.01	0.01	0.38	99.40	0.20	0.01	0.00	0.01	0.01	0.03	0.03	0.74	99.11	0.06	0.07	0.06
	$(0, 2, 2, \frac{3}{2})$	0.00	0.00	98.56	0.37	0.00	0.07	1.41	0.00	0.00	0.00	0.27	0.00	0.07	26.76	72.99	0.00
	$(2, 0, 2, \frac{3}{2})$	0.07	0.06	1.00	0.02	0.35	0.51	97.76	0.06	0.01	0.02	99.57	0.07	0.02	0.04	0.21	0.09
	$(1, 1, 1, \frac{1}{2})$	0.01	0.02	0.03	0.01	0.12	99.22	0.53	0.05	0.00	0.00	0.05	0.02	0.02	73.09	26.72	0.01
	$(2, 2, 1, \frac{1}{2})$	0.00	0.00	0.02	0.00	0.00	0.00	0.00	0.00	0.00	0.00	0.00	0.00	0.00	0.00	0.00	0.00
	$(2, 2, 1, \frac{3}{2})$	0.00	0.00	0.01	0.00	0.00	0.00	0.00	0.00	0.00	0.00	0.00	0.00	0.00	0.00	0.00	0.00
$\frac{3}{2}^+$	$J^P(l, L, L_t, S)$	8030	8469	8545	8549	8603	8622	8660	8670	11221	11627	11700	11708	11752	11813	11827	11837
	$(0, 0, 0, \frac{3}{2})$	99.70	99.38	0.05	0.02	98.35	0.08	0.18	0.08	99.89	99.28	0.07	0.01	99.76	0.06	0.00	0.04
	$(2, 2, 0, \frac{3}{2})$	0.20	0.53	0.00	0.01	1.19	0.00	0.00	0.00	0.09	0.69	0.00	0.00	0.07	0.00	0.00	0.00
	$(0, 2, 2, \frac{3}{2})$	0.01	0.00	53.37	44.20	0.08	0.95	0.06	0.67	0.01	0.01	0.07	0.39	0.00	0.36	21.69	9.58
	$(2, 0, 2, \frac{3}{2})$	0.04	0.04	0.67	0.66	0.03	0.07	8.31	39.60	0.01	0.01	32.86	66.58	0.06	0.03	0.15	0.01
	$(0, 2, 2, \frac{1}{2})$	0.00	0.00	43.57	53.77	0.00	0.60	0.05	1.45	0.00	0.00	0.44	0.44	0.00	0.21	77.54	2.74
	$(1, 1, 2, \frac{1}{2})$	0.00	0.00	1.50	0.00	0.06	98.29	0.01	0.10	0.00	0.00	0.12	0.00	0.05	99.13	0.01	0.02
	$(2, 0, 2, \frac{1}{2})$	0.03	0.03	0.79	1.18	0.15	0.00	2.13	57.54	0.00	0.01	66.43	32.57	0.02	0.08	0.61	0.01
	$(1, 1, 1, \frac{1}{2})$	0.01	0.02	0.01	0.15	0.12	0.00	89.25	0.55	0.00	0.00	0.01	0.00	0.02	0.13	0.00	87.59
	$(2, 2, 1, \frac{1}{2})$	0.00	0.00	0.01	0.00	0.00	0.00	0.00	0.00	0.00	0.00	0.00	0.00	0.00	0.00	0.00	0.00
$\frac{5}{2}^+$	$J^P(l, L, L_t, S)$	8548	8550	8625	8668	8679	8862	8863	8957	11699	11712	11812	11830	11846	11986	11996	12091
	$(0, 2, 2, \frac{3}{2})$	18.23	78.37	1.68	0.57	1.85	28.19	70.13	1.12	0.03	0.70	0.69	54.28	44.48	0.06	0.74	0.03
	$(2, 0, 2, \frac{3}{2})$	0.34	1.52	0.20	19.41	77.78	0.24	0.59	0.44	13.23	86.04	0.01	0.40	0.13	13.60	85.60	0.00
	$(2, 0, 2, \frac{1}{2})$	2.02	0.48	0.37	77.22	19.02	0.82	0.32	0.47	86.16	13.05	0.08	0.32	0.18	85.67	13.46	0.03
	$(1, 1, 2, \frac{1}{2})$	1.65	0.55	96.86	0.15	0.79	0.96	0.20	97.25	0.04	0.01	98.73	1.22	0.00	0.03	0.01	99.88
	$(0, 2, 2, \frac{1}{2})$	77.74	19.06	0.88	2.64	0.56	69.75	28.71	0.69	0.54	0.21	0.49	43.77	55.21	0.64	0.19	0.03
	$(2, 2, 1, \frac{3}{2})$	0.00	0.00	0.00	0.00	0.01	0.01	0.01	0.00	0.00	0.00	0.00	0.00	0.00	0.00	0.00	0.00
	$(2, 2, 3, \frac{3}{2})$	0.01	0.00	0.00	0.00	0.00	0.01	0.00	0.01	0.00	0.00	0.00	0.00	0.00	0.00	0.00	0.00
	$(1, 3, 3, \frac{1}{2})$	0.00	0.01	0.00	0.00	0.00	0.02	0.04	0.00	0.00	0.00	0.00	0.00	0.00	0.00	0.00	0.00
	$(2, 2, 3, \frac{1}{2})$	0.00	0.01	0.00	0.00	0.00	0.00	0.01	0.01	0.00	0.00	0.00	0.00	0.00	0.00	0.00	0.00
	$(3, 1, 3, \frac{1}{2})$	0.00	0.00	0.00	0.00	0.00	0.00	0.00	0.00	0.00	0.00	0.00	0.00	0.00	0.00	0.00	0.02
$\frac{7}{2}^+$	$J^P(l, L, L_t, S)$	8552	8676	8866	8985	9029	9033	9080	9087	11715	11833	11998	12160	12174	12189	12198	12236
	$(0, 2, 2, \frac{3}{2})$	97.70	3.16	98.78	73.97	22.35	4.45	0.02	0.03	0.97	99.25	0.97	97.20	0.05	25.72	76.22	0.00
	$(2, 0, 2, \frac{3}{2})$	2.28	96.84	1.15	25.52	68.46	5.22	1.05	0.99	99.03	0.74	99.03	2.80	0.65	73.50	23.67	0.04
	$(2, 2, 3, \frac{3}{2})$	0.00	0.00	0.01	0.00	0.04	1.82	30.45	64.35	0.00	0.00	0.00	0.00	0.04	0.11	0.03	59.84
	$(1, 3, 3, \frac{1}{2})$	0.01	0.00	0.06	0.49	8.96	87.47	0.02	2.62	0.00	0.00	0.00	0.00	0.19	0.00	0.00	0.10
	$(2, 2, 3, \frac{1}{2})$	0.00	0.00	0.00	0.00	0.07	0.47	68.46	30.35	0.00	0.00	0.00	0.00	0.01	0.02	0.01	39.98
	$(3, 1, 3, \frac{1}{2})$	0.00	0.00	0.00	0.00	0.11	0.58	0.00	1.66	0.00	0.00	0.00	0.00	99.05	0.65	0.06	0.04
	$J^P(l, L, L_t, S)$	8310	8319	8389	8668	8675	8771	8809	8813	11496	11559	11571	11823	11915	11919	11971	11977
$\frac{1}{2}^-$	$(0, 1, 1, \frac{1}{2})$	20.76	79.21	0.04	22.25	77.66	0.15	66.10	33.28	0.23	9.02	90.75	0.08	10.65	89.28	12.02	87.47
	$(1, 0, 1, \frac{1}{2})$	0.02	0.01	99.92	0.09	0.03	99.67	0.89	0.01	99.41	0.52	0.07	99.81	0.15	0.03	0.90	0.16
	$(2, 0, 1, \frac{1}{2})$	79.20	20.77	0.04	77.63	22.31	0.15	32.93	66.72	0.36	90.45	9.18	0.11	89.20	10.69	87.07	12.37
	$(2, 1, 2, \frac{1}{2})$	0.03	0.01	0.00	0.03	0.01	0.03	0.09	0.00	0.00	0.00	0.00	0.00	0.00	0.01	0.00	0.00
	$J^P(l, L, L_t, S)$	8322	8323	8397	8677	8678	8746	8777	8808	11506	11576	11578	11830	11922	11928	11980	11981
	$(0, 1, 1, \frac{1}{2})$	85.60	14.04	0.29	94.30	5.51	0.00	0.12	96.51	0.06	33.20	66.73	0.02	55.74	44.22	13.84	35.70
	$(1, 0, 1, \frac{1}{2})$	0.54	0.13	99.33	0.17	0.13	0.00	99.68	0.13	99.93	0.02	0.04	99.97	0.01	0.01	0.11	0.11
$\frac{3}{2}^-$	$(0, 1, 1, \frac{3}{2})$	13.81	85.78	0.37	5.46	94.31	0.00	0.18	2.78	0.00	66.78	33.22	0.00	44.23	55.76	17.16	33.35
	$(0, 3, 3, \frac{3}{2})$	0.00	0.00	0.00	0.00	0.00	98.19	0.00	0.00	0.00	0.00	0.00	0.00	0.00	0.00	0.00	0.28
	$(2, 1, 3, \frac{3}{2})$	0.02	0.03	0.00	0.03	0.02	1.51	0.00	0.17	0.00	0.00	0.00	0.00	0.00	0.00	0.00	0.00
	$(1, 2, 2, \frac{1}{2})$	0.00	0.00	0.00	0.03	0.01	0.28	0.00	0.39	0.00	0.00	0.00	0.00	0.00	0.00	0.00	0.01
	$(2, 1, 2, \frac{1}{2})$	0.00	0.02	0.00	0.00	0.02	0.00	0.01	0.00	0.00	0.00	0.00	0.00	0.00	0.00	0.00	0.41
	$(2, 1, 2, \frac{3}{2})$	0.02	0.00	0.00	0.02	0.01	0.01	0.01	0.03	0.00	0.00	0.00	0.00	0.00	0.00	0.00	0.01
	$J^P(l, L, L_t, S)$	8330	8684	8743	8747	8811	8818	8856	8863	11584	11878	11927	11975	11982	11987	12014	12018
	$(0, 1, 1, \frac{3}{2})$	99.93	99.89	0.01	0.01	99.08	0.26	0.58	0.00	99.99	0.01	99.95	0.00	0.69	99.17	0.16	0.01
$\frac{5}{2}^-$	$(0, 3, 3, \frac{1}{2})$	0.00	0.00	45.18	51.69	0.00	1.08	0.21	1.94	0.00	0.00	0.00	1.25	0.05	0.00	0.00	0.03
	$(1, 2, 3, \frac{1}{2})$	0.00	0.00	2.24	0.01	0.22	88.07	0.01	2.20	0.00	0.90	0.00	0.00	0.05	0.00	0.14	0.00
	$(2, 1, 3, \frac{1}{2})$	0.03	0.03	0.95	1.09	0.09	0.53	12.64	61.73	0.00	0.09	0.00	88.82	9.09	0.07	0.07	0.03
	<math																

by using harmonic oscillator expansion in Ref. [26], but there is a defect. In principle, the level structures of Ω_{ccc} and Ω_{bbb} baryons should be exactly the same, that is, the order of each state will not change. However, for the mass spectra of Ω_{ccc} and Ω_{bbb} baryons calculated in Ref. [26], the mass of D -wave Ω_{ccc} baryon with $J^P = \frac{1}{2}^+$ is higher than that of S -wave Ω_{ccc} baryon, while for the Ω_{bbb} baryons, it is the opposite, which indicates that the harmonic oscillator expansion method has defects. Our calculation results show that the energy level order of Ω_{ccc} and Ω_{bbb} is exactly the same.

2. Ω_{bcc} and Ω_{bbc} baryons

The lower panel of Fig. 2 presents our predicted mass spectra for Ω_{bcc} and Ω_{bbc} baryons across various quantum states ($J^P = \frac{1}{2}^\pm, \frac{3}{2}^\pm, \frac{5}{2}^\pm, \frac{7}{2}^+$). Our calculations yield masses for the lowest $\frac{1}{2}^+$ and $\frac{3}{2}^+$ states that are slightly elevated (by 10–15 MeV) compared to lattice QCD results [32–34], though still consistent within theoretical uncertainties (see Table V).

While Ω_{bcc} and Ω_{bbc} share similar symmetry properties, their distinct quark compositions (“one heavy + two light” versus “two heavy + one light”) lead to characteristic spectral differences:

- $\frac{1}{2}^+$ system: Contains the ground states ($1S$), followed by $2S$, $3S$, and four distinct D -wave excitations. The state ordering differs between Ω_{bcc} and Ω_{bbc} due to mass effects (Table IV).
- $\frac{3}{2}^+$ system: Features $1S/2S$ states (shifted ~ 20 MeV higher than $\frac{1}{2}^+$), followed by mode-specific $1D$ excitations:
 - Ω_{bcc} : $(0, 2, 2)$ -mode doublet
 - Ω_{bbc} : $(2, 0, 2)$ -mode doublet

Higher states include $3S$ and three $2D$ configurations.

- $\frac{5}{2}^+$ system: Dominated by $1D$ spin doublets with:
 - Ω_{bcc} : $(0, 2, 2)$ -mode doublet
 - Ω_{bbc} : $(2, 0, 2)$ -mode doublet

plus three higher $2D$ states.

- $\frac{7}{2}^+$ system: Contains only $S = 3/2$ D -wave states:
 - Ω_{bcc} : $(0, 2, 2)$ - $1D$ and $(2, 0, 2)$ - $2D$
 - Ω_{bbc} : $(2, 0, 2)$ - $1D$ and $(0, 2, 2)$ - $2D$

Here, we can clearly see the mixing of $(0, 2, 2)$ -mode and $(2, 0, 2)$ -mode, as predicted before.

- $\frac{1}{2}^-$ system: Shows clear P -wave structures with mode-dependent ordering
- $\frac{3}{2}^-$ system: Similar to $\frac{1}{2}^-$ but with ~ 10 MeV mass shifts
- $\frac{5}{2}^-$ system: Ω_{bcc} exhibits two P -wave states while Ω_{bbc} shows a P -wave state and an F -wave state

Prior research primarily considered only λ -mode excitation [67, 68], or posited that mode excitation is dominated by heavy quarks [29]. However, we propose that all distinct mode excitations coexist. Within the established theoretical framework, it is not feasible to selectively exclude any specific mode. These systematic spectral patterns, detailed in Table IV, arise from the interplay between quark masses and QCD dynamics.

TABLE V. Comparison of our results with other studies, including the latest lattice QCD results [4793(5)(7) MeV and 5094(12)(13) MeV for $\frac{3}{2}^+$ and $\frac{3}{2}^-$ states] from Ref. [30].

J^P	Ω_{ccc}		Ω_{bbb}	
	Our	Lattice [31]	Our	Lattice [35, 36]
$\frac{1}{2}^+$	5354	5399(13)	14882	14938(14)(12)
	5370	5405(14)	14898	14953(13)(13)
	5701	6039(33)	15170	
	5719	6083(42)	15190	
	5784	6468(80)	15257	
	5851	6712(56)	15324	
$\frac{3}{2}^+$	4793	4763(6)	14365	14371(4)(11)
	5269	5317(31)	14792	14840(11)(9)
	5372	5430(13)	14901	14958(13)(12)
	5409	5465(13)	14937	15005(14)(13)
	5650	6094(40)	15117	
	5722	6623(46)	15192	
$\frac{5}{2}^+$	5740	6641(43)	15209	
	5796	6741(46)	15266	
	5374	5406(15)	14903	14964(13)(12)
	5409	5464(15)	14937	15007(14)(13)
	5378	5397(49)	14905	14969(12)(12)
	5121	5120(9)	14687	14706.3(5.8)(7.4)
$\frac{7}{2}^-$	5516	5612(31)	15021	
	5552	5631(43)	15041	
	5644	5749(21)	15143	
	5854	6132(69)	15299	
	5136	5124(13)	14692	14714.0(5.5)(7.2)
	5527	5662(31)	15025	
$\frac{3}{2}^-$	5548	5724(44)	15041	
	5629	5765(34)	15123	
	5640	6299(44)	15143	
	5683	6326(51)	15180	
	5547	5516(64)	15042	
	5592	5709(25)	15093	
$\frac{5}{2}^-$	5632	5710(24)	15124	
	5674	5712(32)	15180	
Hadrons				
$\Omega_{bcc}(1/2^+)$	8017	8005(6)(11)	8007(9)(20)	7984(27)(12)
$\Omega_{bcc}(3/2^+)$	8030	8026(7)(11)	8037(9)(20)	8012.8(5.6)(2.2)
$\Omega_{bcc}(3/2^-)$	8322	–	–	8461.8(41)(34)
$\Omega_{bbc}(1/2^+)$	11204	11194(5)(12)	11195(8)(20)	11182(27)(13)
$\Omega_{bbc}(3/2^+)$	11221	11211(6)(12)	11229(8)(20)	11203.8(7.0)(1.7)
$\Omega_{bbc}(1/2^-)$	11496	–	–	11557(74)(28)
$\Omega_{bbc}(3/2^-)$	11506	–	–	11587(12)(2)
$\Omega_{bbb}(3/2^+)$	14365	–	14366(9)(20)	14369(21)(14)

B. Radiative decay

Table VI presents the strong decay thresholds for triply heavy baryons. Our analysis reveals many states lying below these thresholds, making them prime candidates for radiative transitions. We have systematically calculated the radiative decay properties of Ω_{ccc} , Ω_{bbb} , Ω_{bcc} , and Ω_{bbc} baryons with masses below 5.486 GeV ($\Xi_{cc}^{++}D^0$ threshold), 15.25 GeV, 8.58 GeV and 11.72 GeV, respectively. All considered initial states lie below the strong decay threshold, precluding OZI-allowed two-body strong decays. Consequently, these radiative transitions may serve as crucial signatures for identifying these states in future experiments.

TABLE VI. Strong decay thresholds (mass values in MeV) for triply heavy baryons. Masses of Ξ_{cb}^+ and Ξ_{bb}^0 use latest lattice results: 6945(22)(14) MeV [32] and 10143(30)(23) MeV [33].

Ω_{ccc}	Ω_{bcc}	Ω_{bbc}	Ω_{bbb}
$\Xi_{cc}^{++}D^0 : 5486$	$\Xi_{cb}^+ D^0 : 8810$	$\Xi_{bb} D^0 : 12008$	$\Xi_{bb} B^- : 15422$
	$\Xi_{cc}^{++} B^- : 8901$	$\Xi_{cb}^+ B^- : 12224$	

Through our calculations and comparison with previous studies, we have identified two fundamental patterns governing radiative decays in our model:

1. **Three identical quarks:** Radiative transitions between states with conserved parity ($P_i = P_f$) and total spin ($S_i = S_f$) typically exhibit larger partial widths.
2. **Two identical quarks:** The dominant transitions occur between states with conserved total spin ($S_i = S_f$) but flipped parity ($P_i = -P_f$), yielding larger partial widths.

The process of total spin invariance leads to electrical transitions, hence tending to have a larger width. The above two patterns indicate that the influence of identical particle symmetry on baryon radiative decay is significant. For Ω_{ccc} and Ω_{bbb} baryons, the radiative decay width from D -wave to S -wave, F -wave to P -wave, etc. is larger, while for Ω_{bcc} and Ω_{bbc} baryons, the width from P -wave to S -wave, D -wave to P -wave, etc. is larger. The radiative decay width is primarily determined by the total orbital angular momenta L_t of the initial and final states. Therefore, we denote transitions from an X -wave baryon to a Y -wave baryon as $X \rightarrow Y$, where X and Y represent the respective orbital angular momentum states of the particles.

1. The Ω_{ccc} baryons

Table VII presents the radiative decay widths for Ω_{ccc} baryons below the $\Xi_{cc}^{++}D^0$ threshold. Our calculations reveal several key features:

- $S \rightarrow S$ transitions: The two S -wave states $\Omega_{ccc}(5354)1/2^+$ and $\Omega_{ccc}(5269)3/2^+$ decay to the ground state with relatively small decay width 4.99 keV and 0.68 keV.

- $D \rightarrow S$ transitions: Transitions to the ground state $\Omega_{ccc}(4793)3/2^+$ with $S = 3/2$ D -wave initial states exhibit particularly large partial widths, all in the hundreds of keV. The widths of the two $S = 1/2$ D -wave states are only 9.96 keV and 24.68 keV due to the absence of electrical transitions.
- $P \rightarrow S$ transitions: The P -wave states $\Omega_{ccc}(5121)1/2^-$ and $\Omega_{ccc}(5136)3/2^-$ decay to the ground state with widths of $\mathcal{O}(1)$ keV, which is consistent with Ref. [26].
- $X \rightarrow P$ transitions (X stands for any particle): Processes with P -wave or higher excited final states generally yield smaller widths compared to those with S -wave final states.

It can be observed that our partial calculations differ significantly from those in Ref. [26]. We attribute this discrepancy to two main factors: (1) Ref. [26] does not account for the symmetry of three identical particles; (2) the potential models employed differ between the studies. Notably, the results obtained in Ref. [26] are consistent with the radiative decay characteristics of two-identical-quark baryons.

2. The Ω_{bbb} baryons

Table VIII presents radiative decay widths for Ω_{bbb} baryons with masses below 15.25 GeV. These widths are generally smaller than those of Ω_{ccc} baryons due to differences in both quark charge and mass between the b and c quarks. Many transitions are negligible (0.00 keV). The well-resolved mass spectrum of these three-identical-particle systems facilitates comprehensive calculation of radiative widths for nearly all Ω_{bbb} states shown in Fig. 2. Key observations include:

- $S \rightarrow S$ transitions: The transitions from S -wave to S -wave are relatively small, only 0.01 keV.
- $D \rightarrow S$ transitions: Similar to Ω_{ccc} cases, the larger partial widths occur for D -wave to S -wave transitions with conserved total spin, while the processes of total spin change are two orders of magnitude less.
- $P \rightarrow S$ transitions: The transitions of total spin varying from P -wave to S -wave are small, only 0.03 keV, but the total spin invariant processes are 5 to 6 times that of them.
- $X \rightarrow P$ transitions: For decays to P -wave final states
 - The transition $\Omega_{bbb}(15093)5/2^- \rightarrow \Omega_{bbb}(14687)1/2^-\gamma$ is enhanced due to the F -wave nature of the initial state.
 - Negative-parity initial states show stronger transitions to $\Omega_{bbb}(14692)3/2^-\gamma$.
- $D \rightarrow 2S$ transitions: Higher excited D -wave to $2S$ -wave transitions remain significant.

Transitions to higher excited states exhibit systematically smaller widths, as shown in the table. However, there remain order-of-magnitude discrepancies between our results and those of Ref. [26], which can be attributed to similar reasons as in the case of Ω_{ccc} .

3. The Ω_{bcc} baryons

The radiative decay widths of Ω_{bcc} baryons below the 8.58 GeV are presented in Table IX. Unlike the Ω_{ccc} and Ω_{bbb} systems composed of three identical quarks, Ω_{bcc} baryons exhibit distinct symmetry properties that lead to characteristic radiative decay patterns. Both $\frac{1}{2}^+$ and $\frac{3}{2}^+$ channels contain low-lying states ($\Omega_{bcc}(8017)1/2^+$ and $\Omega_{bcc}(8030)3/2^+$) that serve as dominant final states.

The radiative decays of the Ω_{bcc} baryons show several notable features:

- $S \rightarrow S$ transitions: The $S \rightarrow S$ transitions for the Ω_{bcc} baryons are also weak.
- $D \rightarrow S$ transitions: The processes from D -wave to S -wave yield widths of $O(10)$ keV. The relative widths to $1/2^+$ versus $3/2^+$ S -wave final states depend on total spin of initial and final states. Four $J^P = 3/2^+$ or $5/2^+$ D -wave states show significant $S = 1/2$ - $3/2$ mixing, exhibiting comparable widths to both S -wave final states.
- $P \rightarrow S$ transitions: Five $(0, 1, 1)$ -mode excitations decaying to two S -wave states produce widths of $O(100)$ keV, but two $(1, 0, 1)$ -mode states show suppressed widths (\sim few keV).
- $S \rightarrow P$ transitions: The S -wave state decays to five P -wave states with widths ranging from several to tens of keV.
- $D \rightarrow P$ transitions: The $D \rightarrow P$ transitions follow a clear angular momentum hierarchy:
 - $|J_i - J_f| = 1$: largest widths (diagonal elements)
 - $|J_i - J_f| > 1$: negligible (left of diagonal)
 - $|J_i - J_f| < 1$: intermediate (right of diagonal)

The results above adequately demonstrate the radiative decay characteristic of two-identical-quark baryon, which is far different from three-identical-quark baryon.

4. The Ω_{bbc} baryons

The radiative decay widths of the Ω_{bbc} baryons below and 11.72 GeV are shown in Table IX. Compared to the Ω_{bcc} baryons, the radiative decay widths of the Ω_{bbc} baryons is generally smaller, and the processes with $1S$ state as the final state have a larger partial width. This may be due to the smaller charge and larger mass of b quark.

The radiative decays of the Ω_{bbc} baryons reveal:

- $S, D \rightarrow S$ transitions: The radiative decay widths are generally small, typically only a few tenths of keV.
- $P \rightarrow S$ transitions: Similar to the Ω_{bcc} baryons, the widths of the five $(0, 1, 1)$ -mode excitations are $O(100)$ keV, whereas the widths of the two $(1, 0, 1)$ -mode excitations are only a few tenths of keV.

Due to identical particle symmetry, the radiative decay behavior of Ω_{bbc} closely resembles that of Ω_{bcc} . However, differences in the energy level structure—caused by the constituent quark mass (i.e., “one heavy + two light” versus “two heavy + one light”)—may introduce slight variations in their radiative decay behaviors.

IV. SUMMARY

Within the framework of the nonrelativistic quark model, we have systematically investigated the mass spectra of triply heavy baryons up to D -wave states using the Gaussian expansion method. Subsequently, the radiative decay widths for states up to $1D$ were calculated utilizing the wave functions obtained from the mass spectrum computations.

Key findings regarding the spectroscopic properties, as elaborated in preceding sections, are summarized as follows:

- **Ω_{ccc} and Ω_{bbb} baryons:**
 1. Predicted masses for low-lying states agree with lattice QCD results, while those for excited states are generally lower—a trend consistent with most potential model predictions.
 2. We establish that $J^P = 1/2^+$ baryons composed of three identical quarks still possess S -wave bound states, correcting a misinterpretation in earlier literature.
- **Ω_{bcc} and Ω_{bbc} baryons:**
 1. Our calculated mass spectra are consistent with lattice results within their respective uncertainties.
 2. We demonstrate the existence of all excitation modes for baryons with two identical quarks, with certain modes exhibiting mixing effects. This contrasts with approaches in other works that explicitly exclude specific modes.

The predicted spectra await experimental verification, particularly at future heavy-quark production facilities.

For radiative decays, the principal conclusions are:

1. Radiative decay patterns differ fundamentally between baryons with three identical quarks and those with two identical quarks, governed by distinct underlying mechanisms.
2. Our calculated radiative decay widths for Ω_{ccc} and Ω_{bbb} baryons exhibit discrepancies with Ref. [26], likely attributable to its omission of identical particle symmetry considerations.

TABLE VII. Radiative decay widths (in keV) for Ω_{ccc} baryons with masses below the $\Xi_{cc}^{++}D^0$ threshold. Residual radiative decay widths for Ω_{ccc} baryons not tabulated are all below 0.005 keV.

(L_t, S)	Initial state	$\Omega_{ccc}(4793) 3/2^+\gamma$		$\Omega_{ccc}(5121) 1/2^-\gamma$		$\Omega_{ccc}(5136) 3/2^-\gamma$		$\Omega_{ccc}(5269) 3/2^+\gamma$
		Our	Ref. [26]	Our	Ref. [26]	Our	Ref. [26]	
$(0, \frac{1}{2})$	$\Omega_{ccc}(5354) 1/2^+$	4.99	-	0.18	20.14	0.50	27.43	$\Omega_{ccc}(5370) 1/2^+$
$(0, \frac{3}{2})$	$\Omega_{ccc}(5269) 3/2^+$	0.68	-	0.02	0.002	0.03	0.010	$\Omega_{ccc}(5372) 3/2^+$
$(2, \frac{1}{2})$	$\Omega_{ccc}(5409) 3/2^+$	9.96	-	0.43	106.88	1.33	33.58	$\Omega_{ccc}(5374) 5/2^+$
	$\Omega_{ccc}(5409) 5/2^+$	24.68	-	0.47	0.25	0.94	122.10	$\Omega_{ccc}(5378) 7/2^+$
$(2, \frac{3}{2})$	$\Omega_{ccc}(5370) 1/2^+$	176.94	-	0.14	<0.001	0.07	0.04	$\Omega_{ccc}(5409) 3/2^+$
	$\Omega_{ccc}(5372) 3/2^+$	162.60	-	0.58	0.38	0.02	0.02	$\Omega_{ccc}(5409) 5/2^+$
	$\Omega_{ccc}(5374) 5/2^+$	132.83	-	0.36	0.22	0.22	0.39	$\Omega_{ccc}(5378) 7/2^+$
$(1, \frac{1}{2})$	$\Omega_{ccc}(5378) 7/2^+$	138.47	-	0.00	<0.001	0.39	0.80	$\Omega_{ccc}(5409) 3/2^+ \rightarrow \Omega_{ccc}(5354) 1/2^+\gamma$
	$\Omega_{ccc}(5121) 1/2^-$	2.52	3.10	-	-	-	-	$\Omega_{ccc}(5409) 5/2^+ \rightarrow \Omega_{ccc}(5372) 3/2^+\gamma$
	$\Omega_{ccc}(5136) 3/2^-$	3.05	4.07	0.00	-	-	-	$\Omega_{ccc}(5409) 5/2^+ \rightarrow \Omega_{ccc}(5378) 7/2^+\gamma$

TABLE VIII. The radiative decay widths for Ω_{bbb} baryons with masses below 15.25 GeV (in keV). Residual radiative decay widths for Ω_{bbb} baryons not tabulated are all below 0.005 keV.

(L_t, S)	Initial state	$\Omega_{bbb}(14365) 3/2^+\gamma$		$\Omega_{bbb}(14687) 1/2^-\gamma$		$\Omega_{bbb}(14792) 3/2^+\gamma$	
		Our	Ref. [26]	$\Omega_{bbb}(15170) 1/2^+$	0.02	$\Omega_{bbb}(14898) 1/2^+$	0.01
$(0, \frac{1}{2})$	$\Omega_{bbb}(14882) 1/2^+$	0.01	-	$\Omega_{bbb}(15209) 3/2^+$	0.03	$\Omega_{bbb}(14901) 3/2^+$	0.01
	$\Omega_{bbb}(15170) 1/2^+$	0.01	-	$\Omega_{bbb}(15211) 5/2^+$	0.02	$\Omega_{bbb}(14903) 5/2^+$	0.01
	$\Omega_{bbb}(14937) 3/2^+$	0.01	-	$\Omega_{bbb}(15180) 3/2^-$	0.88	$\Omega_{bbb}(14905) 7/2^+$	0.01
$(2, \frac{1}{2})$	$\Omega_{bbb}(14937) 5/2^+$	0.03	-	$\Omega_{bbb}(15143) 3/2^-$	0.68	$\Omega_{bbb}(15190) 1/2^+$	2.49
	$\Omega_{bbb}(15209) 3/2^+$	0.01	-	$\Omega_{bbb}(15025) 3/2^-$	0.42	$\Omega_{bbb}(15192) 3/2^+$	2.44
$(2, \frac{3}{2})$	$\Omega_{bbb}(15211) 5/2^+$	0.03	-	$\Omega_{bbb}(15180) 5/2^-$	0.33	$\Omega_{bbb}(15194) 5/2^+$	2.35
	$\Omega_{bbb}(14898) 1/2^+$	4.63	-	$\Omega_{bbb}(15093) 5/2^-$	3.69	$\Omega_{bbb}(15196) 7/2^+$	2.27
$(1, \frac{1}{2})$	$\Omega_{bbb}(14901) 3/2^+$	4.56	-	$\Omega_{bbb}(14692) 3/2^-\gamma$		$\Omega_{bbb}(15211) 5/2^+$	0.01
	$\Omega_{bbb}(14903) 5/2^+$	4.45	-	Our	Ref. [26]	$\Omega_{bbb}(15021) 1/2^-$	0.01
$(1, \frac{3}{2})$	$\Omega_{bbb}(14905) 7/2^+$	4.37	-	$\Omega_{bbb}(15170) 1/2^+$	0.02	$\Omega_{bbb}(15025) 3/2^-$	0.01
	$\Omega_{bbb}(15190) 1/2^+$	2.81	-	$\Omega_{bbb}(14937) 3/2^+$	0.01	$\Omega_{bbb}(15123) 3/2^-$	0.02
$(1, \frac{3}{2})$	$\Omega_{bbb}(15192) 3/2^+$	2.84	-	$\Omega_{bbb}(15209) 3/2^+$	0.03	$\Omega_{bbb}(15124) 5/2^-$	0.02
	$\Omega_{bbb}(15194) 5/2^+$	2.84	-	$\Omega_{bbb}(15211) 5/2^+$	0.09	$\Omega_{bbb}(14882) 1/2^+\gamma$	
$(3, \frac{3}{2})$	$\Omega_{bbb}(15196) 7/2^+$	2.87	-	$\Omega_{bbb}(15143) 1/2^-$	1.43	$\Omega_{bbb}(15143) 1/2^-$	0.01
	$\Omega_{bbb}(14687) 1/2^-$	0.02	0.035	$\Omega_{bbb}(15021) 1/2^-$	0.76	$\Omega_{bbb}(15209) 3/2^+$	1.02
$(1, \frac{1}{2})$	$\Omega_{bbb}(14692) 3/2^-$	0.03	0.038	$\Omega_{bbb}(15180) 3/2^-$	0.98	$\Omega_{bbb}(15211) 5/2^+$	1.02
	$\Omega_{bbb}(15021) 1/2^-$	0.03	-	$\Omega_{bbb}(15143) 3/2^-$	0.64	$\Omega_{bbb}(14898) 1/2^+\gamma$	
$(1, \frac{3}{2})$	$\Omega_{bbb}(15025) 3/2^-$	0.03	-	$\Omega_{bbb}(15025) 3/2^-$	0.40	$\Omega_{bbb}(15117) 3/2^+$	0.05
	$\Omega_{bbb}(15041) 1/2^-$	0.14	-	$\Omega_{bbb}(15180) 5/2^-$	1.37	$\Omega_{bbb}(15192) 3/2^+$	0.20
$(3, \frac{3}{2})$	$\Omega_{bbb}(15041) 3/2^-$	0.13	-	$\Omega_{bbb}(15093) 5/2^-$	1.00	$\Omega_{bbb}(15194) 5/2^+$	0.06
	$\Omega_{bbb}(15042) 5/2^-$	0.12	-				
	$\Omega_{bbb}(15123) 3/2^-$	0.36	-				
	$\Omega_{bbb}(15124) 5/2^-$	0.35	-				
$\Omega_{bbb}(14901) 3/2^+\gamma$		$\Omega_{bbb}(14903) 5/2^+\gamma$		$\Omega_{bbb}(14903) 5/2^+\gamma$		$\Omega_{bbb}(14905) 7/2^+\gamma$	
$\Omega_{bbb}(15117) 3/2^+$		$\Omega_{bbb}(15117) 3/2^+$		$\Omega_{bbb}(15117) 3/2^+$		$\Omega_{bbb}(15117) 3/2^+$	
$\Omega_{bbb}(15190) 1/2^+$		$\Omega_{bbb}(15190) 1/2^+$		$\Omega_{bbb}(15190) 1/2^+$		$\Omega_{bbb}(15190) 1/2^+$	
$\Omega_{bbb}(15194) 5/2^+$		$\Omega_{bbb}(15194) 5/2^+$		$\Omega_{bbb}(15194) 5/2^+$		$\Omega_{bbb}(15194) 5/2^+$	
$\Omega_{bbb}(15196) 7/2^+$		$\Omega_{bbb}(15196) 7/2^+$		$\Omega_{bbb}(15196) 7/2^+$		$\Omega_{bbb}(15196) 7/2^+$	
$\Omega_{bbb}(14937) 3/2^+\gamma$		$\Omega_{bbb}(14937) 5/2^+\gamma$		$\Omega_{bbb}(14937) 5/2^+\gamma$		$\Omega_{bbb}(15117) 3/2^+\gamma$	
$\Omega_{bbb}(15170) 1/2^+$		$\Omega_{bbb}(15170) 1/2^+$		$\Omega_{bbb}(15170) 1/2^+$		$\Omega_{bbb}(15194) 5/2^+$	
$\Omega_{bbb}(15209) 3/2^+$		$\Omega_{bbb}(15209) 3/2^+$		$\Omega_{bbb}(15209) 3/2^+$		$\Omega_{bbb}(15196) 7/2^+$	
$\Omega_{bbb}(15211) 5/2^+$		$\Omega_{bbb}(15211) 5/2^+$		$\Omega_{bbb}(15211) 5/2^+$		$\Omega_{bbb}(15196) 7/2^+$	

3. Mixing between the total spin states $S = 1/2$ and $S = 3/2$ plays a crucial role in electric dipole transitions. Consequently, accounting for this mixing is essential for accurate radiative decay width calculations.

We anticipate that our radiative decay predictions will provide valuable guidance for future experiments, enabling verification of decay behaviors governed by distinct symmetry principles.

TABLE IX. The radiative decay widths of the Ω_{bcc} baryons below 8.58 GeV and the Ω_{bbc} baryons below 11.72 GeV in units of keV. All unlisted decay widths for these states are below 0.05 keV.

(L_t, S)	Initial state	$\Omega_{bcc}(8017) 1/2^+ \gamma$	$\Omega_{bcc}(8030) 3/2^+ \gamma$	(L_t, S)	Initial state	$\Omega_{bbc}(11204) 1/2^+ \gamma$	$\Omega_{bbc}(11221) 3/2^+ \gamma$		
$(0, \frac{1}{2})$	$\Omega_{bcc}(8463) 1/2^+$	0.2	0.0	$(0, \frac{3}{2})$	$\Omega_{bbc}(11627) 3/2^+$	0.1	0.0		
	$\Omega_{bcc}(8564) 1/2^+$	0.8	1.1		$\Omega_{bbc}(11700) 3/2^+$	0.7	0.4		
$(0, \frac{3}{2})$	$\Omega_{bcc}(8469) 3/2^+$	0.2	0.2	$(2, \frac{1}{2})$	$\Omega_{bbc}(11699) 5/2^+$	0.9	0.1		
	$\Omega_{bcc}(8549) 3/2^+$	22.9	15.0		$\Omega_{bbc}(11702) 1/2^+$	0.0	1.2		
$(2, \frac{1}{2})$	$\Omega_{bcc}(8548) 5/2^+$	19.1	6.0	$(2, \frac{3}{2})$	$\Omega_{bbc}(11708) 3/2^+$	0.3	0.7		
	$\Omega_{bcc}(8546) 1/2^+$	0.0	31.0		$\Omega_{bbc}(11712) 5/2^+$	0.1	0.7		
$(2, \frac{3}{2})$	$\Omega_{bcc}(8545) 3/2^+$	12.7	15.0		$\Omega_{bbc}(11715) 7/2^+$	0.0	0.8		
	$\Omega_{bcc}(8550) 5/2^+$	4.7	22.6	$(1, \frac{1}{2})$	$\Omega_{bbc}(11571) 1/2^-$	131.7	12.8		
$(1, \frac{1}{2})$	$\Omega_{bcc}(8552) 7/2^+$	0.0	27.7		$\Omega_{bbc}(11578) 3/2^-$	126.3	65.0		
	$\Omega_{bcc}(8319) 1/2^-$	141.5	37.2	$(1, \frac{3}{2})$	$\Omega_{bbc}(11559) 1/2^-$	16.7	147.6		
$(1, \frac{3}{2})$	$\Omega_{bcc}(8322) 3/2^-$	135.9	24.2		$\Omega_{bbc}(11576) 3/2^-$	45.7	98.5		
	$\Omega_{bcc}(8310) 1/2^-$	32.4	122.6	$(1, \frac{1}{2})$	$\Omega_{bbc}(11584) 5/2^-$	0.6	145.3		
$(1, \frac{1}{2})$	$\Omega_{bcc}(8323) 3/2^-$	19.3	134.8		$\Omega_{bbc}(11496) 1/2^-$	0.3	0.4		
	$\Omega_{bcc}(8330) 5/2^-$	0.1	150.9		$\Omega_{bbc}(11506) 3/2^-$	0.1	0.0		
$(1, \frac{1}{2})$	$\Omega_{bcc}(8389) 1/2^-$	1.9	1.9	$\Omega_{bbc}(11627) 3/2^+ \rightarrow \Omega_{bbc}(11559) 1/2^- \gamma$					
	$\Omega_{bcc}(8397) 3/2^-$	2.9	6.1	$\Omega_{bbc}(11621) 1/2^+ \rightarrow \Omega_{bbc}(11571) 1/2^- \gamma$					
$\Omega_{bcc}(8545) 3/2^+ \rightarrow \Omega_{bcc}(8389) 1/2^- \gamma$						0.1			
$\Omega_{bcc}(8546) 1/2^+ \rightarrow \Omega_{bcc}(8389) 1/2^- \gamma$						0.1			
$\Omega_{bcc}(8564) 1/2^+ \rightarrow \Omega_{bcc}(8389) 1/2^- \gamma$						0.1			
$\Omega_{bcc}(8546) 1/2^+ \rightarrow \Omega_{bcc}(8397) 3/2^- \gamma$						0.1			
$\Omega_{bcc}(8546) 1/2^+ \rightarrow \Omega_{bcc}(8397) 3/2^- \gamma$						0.1			
$\Omega_{bcc}(8550) 5/2^+ \rightarrow \Omega_{bcc}(8397) 3/2^- \gamma$						0.1			
$\Omega_{bcc}(8564) 1/2^+ \rightarrow \Omega_{bcc}(8397) 3/2^- \gamma$						25.6			
$\Omega_{bbc}(11700) 3/2^+ \rightarrow \Omega_{bbc}(11496) 1/2^- \gamma$						0.1			
(L_t, S)	Initial state	$\Omega_{bcc}(8310) 1/2^- \gamma$	$\Omega_{bcc}(8319) 1/2^- \gamma$	$\Omega_{bcc}(8322) 3/2^- \gamma$	$\Omega_{bcc}(8323) 3/2^- \gamma$	$\Omega_{bcc}(8330) 5/2^- \gamma$			
$(0, \frac{1}{2}, \frac{3}{2})$	$\Omega_{bcc}(8463) 1/2^+$	5.0	16.0	36.8	6.4	0.0			
	$\Omega_{bcc}(8564) 1/2^+$	0.2	0.5	0.7	1.2	0.1			
$(2, \frac{1}{2}, \frac{3}{2})$	$\Omega_{bcc}(8469) 3/2^+$	9.6	2.1	2.8	18.6	32.1			
	$\Omega_{bcc}(8546) 1/2^+$	146.3	32.3	4.4	29.8	0.0			
$(2, \frac{3}{2}, \frac{3}{2})$	$\Omega_{bcc}(8545) 3/2^+$	98.1	19.3	0.8	68.3	5.4			
	$\Omega_{bcc}(8549) 3/2^+$	1.1	129.3	45.9	23.8	5.3			
$(2, \frac{1}{2}, \frac{1}{2})$	$\Omega_{bcc}(8548) 5/2^+$	0.0	0.2	170.4	0.0	11.5			
	$\Omega_{bcc}(8550) 5/2^+$	0.1	0.0	2.4	133.3	44.2			
$(2, \frac{3}{2}, \frac{1}{2})$	$\Omega_{bcc}(8552) 7/2^+$	0.0	0.0	0.1	0.0	172.1			

ACKNOWLEDGMENTS

This work is supported by the National Natural Science Foundation of China under Grant Nos. 12335001, 12247101, and 12405098, the ‘111 Center’ under Grant No. B20063,

the Natural Science Foundation of Gansu Province (No. 22JR5RA389, No. 25JRRRA799), the Talent Scientific Fund of Lanzhou University, the fundamental Research Funds for the Central Universities (No. lzujbky-2023-stlt01), and the project for top-notch innovative talents of Gansu province.

-
- [1] X. Liu, An overview of XYZ new particles, *Chin. Sci. Bull.* **59**, 3815 (2014).
 - [2] A. Hosaka, T. Iijima, K. Miyabayashi, Y. Sakai, and S. Yasui, Exotic hadrons with heavy flavors: X , Y , Z , and related states, *PTEP* **2016**, 062C01 (2016).
 - [3] H.-X. Chen, W. Chen, X. Liu, and S.-L. Zhu, The hidden-charm pentaquark and tetraquark states, *Phys. Rept.* **639**, 1 (2016).
 - [4] J.-M. Richard, Exotic hadrons: review and perspectives, *Few Body Syst.* **57**, 1185 (2016).
 - [5] S. L. Olsen, T. Skwarnicki, and D. Zieminska, Nonstandard heavy mesons and baryons: Experimental evidence, *Rev. Mod. Phys.* **90**, 015003 (2018).
 - [6] F.-K. Guo, C. Hanhart, U.-G. Meißner, Q. Wang, Q. Zhao, and B.-S. Zou, Hadronic molecules, *Rev. Mod. Phys.* **90**, 015004 (2018), [Erratum: Rev.Mod.Phys. 94, 029901 (2022)].
 - [7] Y.-R. Liu, H.-X. Chen, W. Chen, X. Liu, and S.-L. Zhu, Pentaquark and tetraquark states, *Prog. Part. Nucl. Phys.* **107**, 237 (2019).
 - [8] N. Brambilla, S. Eidelman, C. Hanhart, A. Nefediev, C.-P. Shen, C. E. Thomas, A. Vairo, and C.-Z. Yuan, The XYZ states: experimental and theoretical status and perspectives, *Phys. Rept.* **873**, 1 (2020).
 - [9] L. Meng, B. Wang, G.-J. Wang, and S.-L. Zhu, Chiral perturbation theory for heavy hadrons and chiral effective field theory for heavy hadronic molecules, *Phys. Rept.* **1019**, 1 (2023).
 - [10] H.-X. Chen, W. Chen, X. Liu, Y.-R. Liu, and S.-L. Zhu, An

- updated review of the new hadron states, *Rept. Prog. Phys.* **86**, 026201 (2023).
- [11] R. Aaij *et al.* (LHCb Collaboration), First Observation of the Doubly Charmed Baryon Decay $\Xi_{cc}^{++} \rightarrow \Xi_c^+ \pi^+$, *Phys. Rev. Lett.* **121**, 162002 (2018).
- [12] P. Hasenfratz, R. R. Horgan, J. Kuti, and J. M. Richard, Heavy baryon spectroscopy in the QCD bag model, *Phys. Lett. B* **94**, 401 (1980).
- [13] A. Bernotas and V. Simonis, Heavy hadron spectroscopy and the bag model, *Lith. J. Phys.* **49**, 19 (2009).
- [14] B. Silvestre-Brac, Spectrum and static properties of heavy baryons, *Few Body Syst.* **20**, 1 (1996).
- [15] J. Vijande, H. Garcilazo, A. Valcarce, and F. Fernandez, Spectroscopy of doubly charmed baryons, *Phys. Rev. D* **70**, 054022 (2004).
- [16] S. Migura, D. Merten, B. Metsch, and H.-R. Petry, Charmed baryons in a relativistic quark model, *Eur. Phys. J. A* **28**, 41 (2006).
- [17] Y. Jia, Variational study of weakly coupled triply heavy baryons, *JHEP* **10**, 073.
- [18] A. P. Martynenko, Ground-state triply and doubly heavy baryons in a relativistic three-quark model, *Phys. Lett. B* **663**, 317 (2008).
- [19] W. Roberts and M. Pervin, Heavy baryons in a quark model, *Int. J. Mod. Phys. A* **23**, 2817 (2008).
- [20] B. Patel, A. Majethiya, and P. C. Vinodkumar, Masses and magnetic moments of triply heavy flavour baryons in hypercentral model, *Pramana* **72**, 679 (2009).
- [21] J. M. Flynn, E. Hernandez, and J. Nieves, Triply heavy baryons and heavy quark spin symmetry, *Phys. Rev. D* **85**, 014012 (2012).
- [22] Z. Shah and A. K. Rai, Masses and regge trajectories of triply heavy Ω_{ccc} and Ω_{bbb} baryons, *Eur. Phys. J. A* **53**, 195 (2017).
- [23] X.-Z. Weng, X.-L. Chen, and W.-Z. Deng, Masses of doubly heavy-quark baryons in an extended chromomagnetic model, *Phys. Rev. D* **97**, 054008 (2018).
- [24] S.-X. Qin, C. D. Roberts, and S. M. Schmidt, Poincaré-covariant analysis of heavy-quark baryons, *Phys. Rev. D* **97**, 114017 (2018).
- [25] G. Yang, J. Ping, P. G. Ortega, and J. Segovia, Triply heavy baryons in the constituent quark model, *Chin. Phys. C* **44**, 023102 (2020).
- [26] M.-S. Liu, Q.-F. Lü, and X.-H. Zhong, Triply charmed and bottom baryons in a constituent quark model, *Phys. Rev. D* **101**, 074031 (2020).
- [27] R. N. Faustov and V. O. Galkin, Triply heavy baryon spectroscopy in the relativistic quark model, *Phys. Rev. D* **105**, 014013 (2022).
- [28] E. Ortiz-Pacheco and R. Bijker, Masses and radiative decay widths of S - and P -wave singly, doubly, and triply heavy charm and bottom baryons, *Phys. Rev. D* **108**, 054014 (2023).
- [29] G.-L. Yu, Z.-Y. Li, Z.-G. Wang, and Z. Zhou, Systematic analysis of the mass spectra of triply heavy baryons, *Eur. Phys. J. C* **85**, 543 (2025).
- [30] N. S. Dhindsa, D. Chakraborty, A. Radhakrishnan, N. Mathur, and M. Padmanath, Precise study of triply charmed baryons (Ω_{ccc}), [arXiv:2411.12729 \[hep-lat\]](#).
- [31] M. Padmanath, R. G. Edwards, N. Mathur, and M. Peardon, Spectroscopy of triply-charmed baryons from lattice QCD, *Phys. Rev. D* **90**, 074504 (2014).
- [32] N. Mathur, M. Padmanath, and S. Mondal, Precise predictions of charmed-bottom hadrons from lattice QCD, *Phys. Rev. Lett.* **121**, 202002 (2018).
- [33] Z. S. Brown, W. Detmold, S. Meinel, and K. Orginos, Charmed bottom baryon spectroscopy from lattice QCD, *Phys. Rev. D* **90**, 094507 (2014).
- [34] T. Burch, Heavy hadrons on $N_f = 2$ and $2 + 1$ improved clover-Wilson lattices, [arXiv:1502.00675 \[hep-lat\]](#).
- [35] S. Meinel, Prediction of the Ω_{bbb} mass from lattice QCD, *Phys. Rev. D* **82**, 114514 (2010).
- [36] S. Meinel, Excited-state spectroscopy of triply-bottom baryons from lattice QCD, *Phys. Rev. D* **85**, 114510 (2012).
- [37] C. Alexandrou, S. Bacchio, G. Christou, and J. Finkenrath, Low-lying baryon masses using twisted mass fermions ensembles at the physical pion mass, *Phys. Rev. D* **108**, 094510 (2023).
- [38] J.-B. Li, L.-C. Gui, W. Sun, J. Liang, and W. Qin, Triply charmed baryons mass decomposition from lattice QCD, (2022), [arXiv:2211.04713 \[hep-lat\]](#).
- [39] Y. Lyu, H. Tong, T. Sugiura, S. Aoki, T. Doi, T. Hatsuda, J. Meng, and T. Miyamoto, Dibaryon with highest charm number near unitarity from lattice QCD, *Phys. Rev. Lett.* **127**, 072003 (2021).
- [40] H. Bahtiyar, K. U. Can, G. Erkol, P. Gubler, M. Oka, and T. T. Takahashi, Charmed baryon spectrum from lattice QCD near the physical point, *Phys. Rev. D* **102**, 054513 (2020).
- [41] C. Alexandrou and C. Kallidonis, Low-lying baryon masses using $N_f = 2$ twisted mass clover-improved fermions directly at the physical pion mass, *Phys. Rev. D* **96**, 034511 (2017).
- [42] Y.-C. Chen and T.-W. Chiu (TWQCD Collaboration), Lattice QCD with $N_f = 2 + 1 + 1$ domain-wall quarks, *Phys. Lett. B* **767**, 193 (2017).
- [43] K. U. Can, G. Erkol, M. Oka, and T. T. Takahashi, Look inside charmed-strange baryons from lattice QCD, *Phys. Rev. D* **92**, 114515 (2015).
- [44] C. Alexandrou, V. Drach, K. Jansen, C. Kallidonis, and G. Koutsou, Baryon spectrum with $N_f = 2 + 1 + 1$ twisted mass fermions, *Phys. Rev. D* **90**, 074501 (2014).
- [45] Y. Namekawa *et al.* (PACS-CS), Charmed baryons at the physical point in $2 + 1$ flavor lattice QCD, *Phys. Rev. D* **87**, 094512 (2013).
- [46] S. Durr, G. Koutsou, and T. Lippert, Meson and baryon dispersion relations with Brillouin fermions, *Phys. Rev. D* **86**, 114514 (2012).
- [47] C. Alexandrou, J. Carbonell, D. Christaras, V. Drach, M. Gravina, and M. Papinutto, Strange and charm baryon masses with two flavors of dynamical twisted mass fermions, *Phys. Rev. D* **86**, 114501 (2012).
- [48] R. A. Briceno, H.-W. Lin, and D. R. Bolton, Charmed-baryon spectroscopy from lattice QCD with $N_f = 2 + 1 + 1$ flavors, *Phys. Rev. D* **86**, 094504 (2012).
- [49] T.-W. Chiu and T.-H. Hsieh, Baryon masses in lattice QCD with exact chiral symmetry, *Nucl. Phys. A* **755**, 471 (2005).
- [50] N. Brambilla, A. Vairo, and T. Rosch, Effective field theory Lagrangians for baryons with two and three heavy quarks, *Phys. Rev. D* **72**, 034021 (2005).
- [51] F. J. Llanes-Estrada, O. I. Pavlova, and R. Williams, A First Estimate of Triply Heavy Baryon Masses from the pNRQCD Perturbative Static Potential, *Eur. Phys. J. C* **72**, 2019 (2012).
- [52] J.-R. Zhang and M.-Q. Huang, Deciphering triply heavy baryons in terms of QCD sum rules, *Phys. Lett. B* **674**, 28 (2009).
- [53] Z.-G. Wang, Analysis of the triply heavy baryon states with QCD sum rules, *Commun. Theor. Phys.* **58**, 723 (2012).
- [54] T. M. Aliev, K. Azizi, and M. Savci, Masses and residues of the triply heavy spin-1/2 baryons, *JHEP* **04**, 042.
- [55] T. M. Aliev, K. Azizi, and M. Savci, Properties of triply heavy spin-3/2 baryons, *J. Phys. G* **41**, 065003 (2014).
- [56] K. Azizi, T. M. Aliev, and M. Savci, Properties of doubly and triply heavy baryons, *J. Phys. Conf. Ser.* **556**, 012016 (2014).
- [57] Z.-G. Wang, Analysis of the triply-heavy baryon states with the QCD sum rules, *AAPPS Bull.* **31**, 5 (2021).
- [58] Z. R. Najjar and K. Azizi, Investigation of triply heavy spin-3/2

- baryons in their ground and excited states, arXiv:2504.06822 [hep-ph].
- [59] X.-H. Guo, K.-W. Wei, and X.-H. Wu, Some mass relations for mesons and baryons in Regge phenomenology, *Phys. Rev. D* **78**, 056005 (2008).
- [60] K.-W. Wei, B. Chen, and X.-H. Guo, Masses of doubly and triply charmed baryons, *Phys. Rev. D* **92**, 076008 (2015).
- [61] K.-W. Wei, B. Chen, N. Liu, Q.-Q. Wang, and X.-H. Guo, Spectroscopy of singly, doubly, and triply bottom baryons, *Phys. Rev. D* **95**, 116005 (2017).
- [62] K. Serafin, M. Gómez-Rocha, J. More, and S. D. G lazek, Approximate Hamiltonian for baryons in heavy-flavor QCD, *Eur. Phys. J. C* **78**, 964 (2018).
- [63] P.-L. Yin, C. Chen, G. a. Krein, C. D. Roberts, J. Segovia, and S.-S. Xu, Masses of ground-state mesons and baryons, including those with heavy quarks, *Phys. Rev. D* **100**, 034008 (2019).
- [64] L. X. Gutiérrez-Guerrero, A. Bashir, M. A. Bedolla, and E. Santopinto, Masses of light and heavy mesons and baryons: a unified picture, *Phys. Rev. D* **100**, 114032 (2019).
- [65] M. Gómez-Rocha, J. More, and K. Serafin, Baryon masses estimate in heavy flavor QCD: an effective particle approach to hadron spectra, *Few Body Syst.* **64**, 44 (2023).
- [66] S.-Q. Luo and X. Liu, Newly observed $\Omega_c(3327)$: A good candidate for a D -wave charmed baryon, *Phys. Rev. D* **107**, 074041 (2023).
- [67] S.-Q. Luo and X. Liu, Investigating the spectroscopy behavior of undetected $1F$ -wave charmed baryons, *Phys. Rev. D* **108**, 034002 (2023).
- [68] Y.-X. Peng, S.-Q. Luo, and X. Liu, Refining radiative decay studies in singly heavy baryons, *Phys. Rev. D* **110**, 074034 (2024).
- [69] S.-Q. Luo and X. Liu, Identifying triple-strangeness Ω hyperons in light of recent experimental results, (2025), arXiv:2504.14648 [hep-ph].
- [70] S.-Q. Luo, B. Chen, X. Liu, and T. Matsuki, Predicting a new resonance as charmed-strange baryonic analog of $D_{s0}^*(2317)$, *Phys. Rev. D* **103**, 074027 (2021).
- [71] M. Kamimura, Nonadiabatic coupled-rearrangement-channel approach to muonic molecules, *Phys. Rev. A* **38**, 621 (1988).
- [72] E. Hiyama, Y. Kino, and M. Kamimura, Gaussian expansion method for few-body systems, *Prog. Part. Nucl. Phys.* **51**, 223 (2003).
- [73] E. Hiyama, Gaussian expansion method for few-body systems and its applications to atomic and nuclear physics, *PTEP* **2012**, 01A204 (2012).
- [74] T. Yoshida, E. Hiyama, A. Hosaka, M. Oka, and K. Sadato, Spectrum of heavy baryons in the quark model, *Phys. Rev. D* **92**, 114029 (2015), arXiv:1510.01067 [hep-ph].
- [75] W.-J. Deng, L.-Y. Xiao, L.-C. Gui, and X.-H. Zhong, Radiative transitions of charmonium states in a constituent quark model, arXiv:1510.08269 [hep-ph].
- [76] W.-J. Deng, H. Liu, L.-C. Gui, and X.-H. Zhong, Charmonium spectrum and their electromagnetic transitions with higher multipole contributions, *Phys. Rev. D* **95**, 034026 (2017).
- [77] W.-J. Deng, H. Liu, L.-C. Gui, and X.-H. Zhong, Spectrum and electromagnetic transitions of bottomonium, *Phys. Rev. D* **95**, 074002 (2017).
- [78] S. Capstick and N. Isgur, Baryons in a relativized quark model with chromodynamics, *Phys. Rev. D* **34**, 2809 (1986).
- [79] S. Godfrey and N. Isgur, Mesons in a relativized quark model with chromodynamics, *Phys. Rev. D* **32**, 189 (1985).